

Topics In Heavy Quark Physics

Thesis by

Anton N. Kapustin

In Partial Fulfillment of the Requirements

for the Degree of

Doctor of Philosophy



California Institute of Technology

Pasadena, California

1997

(Submitted May 22, 1997)

Acknowledgements

I thank Steve Frautschi, David Politzer, John Preskill, John Schwarz, Mark Wise, Mina Aganagic, Sergei Cherkis, Hooman Davoudiasl, Martin Gremm, Esko Keski-Vakkuri, Adam Leibovich, Zoltan Ligeti, David Lowe, Costin Popescu, Krishna Rajagopal, Iain Stewart, Helen Tuck, and Eric Westphal for a very friendly atmosphere on the fourth floor of Lauritsen. I am particularly grateful to my advisor John Preskill and to people with whom I collaborated during my stay at Caltech: Doron Gepner, Martin Gremm, Zoltan Ligeti, David Politzer, Sergei Skorik, Mark Wise. Special thanks go to my parents for their constant love and support. Last, but not least, I want to thank Mina Aganagic, Sergei Cherkis, Hooman Davoudiasl, Martin Gremm, Yuri Levin, and Sergei Skorik for helping me to waste my time in the most pleasant way possible: talking to good friends.

Abstract

Heavy Quark Effective Theory (HQET) is reviewed and applied to extracting the fundamental parameters of the Standard Model from experimental data. The main focus is on precision measurements of the Cabibbo-Kobayashi-Maskawa matrix element $|V_{cb}|$, and the charm and bottom quark masses m_c and m_b . We discuss the model-independent extraction of $|V_{cb}|$ from the $B \rightarrow D^* \ell \bar{\nu}$ decay rate and show that the corresponding theoretical uncertainties, although small, cannot be further reduced. The theory of the inclusive $B \rightarrow X_c \ell \bar{\nu}$ decay is described and then used to extract $|V_{cb}|$, m_c , and m_b from the available data. We also determine the HQET parameters $\bar{\Lambda}$ and λ_1 which appear in the expressions for the heavy meson decay rates and the relations between the meson and quark masses. At present, the accuracy of the inclusive measurement of $|V_{cb}|$ is comparable to that from the exclusive $B \rightarrow D^* \ell \bar{\nu}$ decay, but could be improved if the bottom quark mass m_b were known better. We show how this could be accomplished by measuring the photon spectrum in the rare inclusive $B \rightarrow X_s \gamma$ decay.

Contents

Acknowledgements	ii
Abstract	iii
1 Introduction	1
2 Theoretical background	4
2.1 Heavy quark symmetry	4
2.2 Heavy quark expansion	14
2.3 Renormalons as a red herring	19
3 The decay $B \rightarrow D^* \ell \bar{\nu}$ and the precision measurement of V_{cb}	23
3.1 Model-independent predictions for the $B \rightarrow D^* \ell \bar{\nu}$ rate at zero recoil .	23
3.2 Zero recoil sum rules	27
4 The uses of the inclusive $B \rightarrow X_c \ell \bar{\nu}$ decays	39
4.1 The theory of the inclusive $B \rightarrow X_c \ell \bar{\nu}$ decays	39
4.2 Applications	48
5 Photon spectrum in the inclusive $B \rightarrow X_s \gamma$ decay	59
5.1 General setup	59
5.2 Order α_s perturbative corrections	62
5.3 Nonperturbative corrections	65
5.4 Extracting HQET parameters from the moments of the photon spectrum	68
6 Concluding remarks	71
Bibliography	73

List of Figures

2.1	The analytic structure of the time-ordered product of two heavy quark currents.	15
2.2	Diagrams representing the OPE coefficients at the tree level. The coefficient of the unit operator is given by diagram (a). The coefficients of the heavy quark bilinears $\bar{Q}\Gamma_A Q$ can be determined from diagram (b). Wavy lines denote the insertions of the current $\bar{q}\Gamma Q$	17
3.1	The integration contour C in the complex ϵ plane. The cuts extend to $\text{Re } \epsilon \rightarrow \pm\infty$	28
3.2	Feynman diagrams that contribute to the order $\alpha_s(\Delta)$ corrections to the sum rules. The black square indicates insertion of the $b \rightarrow c$ axial or vector current.	32
3.3	Feynman diagrams that determine the order $\alpha_s^2(\Delta)\beta_0$ corrections to the sum rules.	33
3.4	$X^{(\infty)}(\Delta)$ and $Y^{(\infty)}(\Delta)$ for the a) axial, and b) vector coefficients. Thick solid lines are X while thick dashed lines are Y . The thin solid and dashed lines are X and Y to order $\Delta^2/m_{c,b}^2$	34
4.1	(a) The relevant term in the operator product expansion. Wavy lines denote the insertions of left-handed currents. (b) does not contribute to $b \rightarrow c$ decay.	41
4.2	Allowed regions in the $\bar{\Lambda}-\lambda_1$ plane for R_1 and R_2 with $1/m_b^3$ corrections omitted. The bands represent the 1σ statistical errors, while the ellipse is the allowed region taking correlations into account.	52

- 4.3 Extraction of $\bar{\Lambda}, \lambda_1$. Cross and ellipse show the values of $\bar{\Lambda}, \lambda_1$ extracted without $1/m_b^3$ corrections but including the experimental statistical error. Shaded region: Higher order matrix elements estimated by dimensional analysis. Cross-hatched region: $\rho_1 = 0.13\text{GeV}^3, \rho_2 = 0$. 56
- 5.1 The analytic structure of the time-ordered product relevant for the $B \rightarrow X_s \gamma$ decay. The moments of the photon spectrum with lower limit E_0 can be obtained by integrating $T(q \cdot v)$ with an appropriate weight along the contour C 66

List of Tables

2.1	Observed heavy mesons and their assignment to HQS doublets. . . .	9
5.1	Central values of $\delta m_1(x_0)$ and $\delta m_2(x_0)$ for two different values of m_s . $r = 4 \cdot 10^{-4}$ corresponds to $m_s = 100$ MeV, while $r = 1 \cdot 10^{-2}$ corresponds to a constituent quark mass $m_s = 500$ MeV. For $m_b \simeq 4.8$ GeV, $x_0 = 0.91$, $x_0 = 0.83$ and $x_0 = 0.75$ correspond to $E_0 = 2.2$ GeV, $E_0 = 2.0$ GeV and $E_0 = 1.8$ GeV, respectively.	64

Chapter 1 Introduction

“My father and mother were honest, though poor—”

“Skip all that!” cried the Bellman in haste.

“If it once becomes dark, there’s no chance of a Snark—”

“We have hardly a minute to waste!”

Lewis Carroll [1]

The current theory of electroweak and strong interactions (the Standard Model) has been confirmed by numerous experiments and is now regarded as the correct theory of particle interactions in the energy range up to about 100 GeV. Among the many stringent tests it has passed the most spectacular ones were the precision measurements of various observables at LEP, where the predictions of the Standard Model were tested with accuracy of fractions of a percent. In modern parlance, this success is expressed by saying that the low-energy effective Lagrangian (for energies below 100 GeV) is indeed the Lagrangian of the Standard Model. There are reasons to believe that at higher energies new particles and interactions come into play, but their effect on low-energy physics can always be accounted for by adding local operators of dimension higher than four to the Lagrangian. Therefore such effects are suppressed by powers of the scale of new physics.

But knowing the Lagrangian is not the same as being able to make quantitative predictions for physical observables. The dynamics of the Standard Model is so complicated that not even all its qualitative features are understood (e.g., confinement of color.) The problem is that strong interactions become so strong at low energies that fundamental constituents, quarks and gluons, are permanently bound inside hadrons (mesons and baryons). Understanding the properties of hadrons is highly nontrivial, since it requires techniques beyond perturbation theory. (The only available nonperturbative tool, lattice Monte-Carlo simulations, is still in its infancy, despite being

about twenty years old.) This is why theoretical particle physics became an art of finding physical quantities which can be both accurately predicted and at least in principle measured.

Unlike other high arts, however, this art needs a *raison d'être*. One motivation is to be able to confront the Standard Model with experiment and hopefully uncover a more fundamental theory underlying it. For example, the aforementioned confirmation of the Standard Model predictions at LEP has become possible only because it was realized that at high energies the strong interactions become weaker (this is the asymptotic freedom of strong interactions discovered by Gross, Wilczek, and Politzer [2].) Another motivation is the desire to measure the parameters of the Standard Model Lagrangian as accurately as possible. There are about twenty such parameters (quark and lepton Yukawa couplings, gauge couplings, etc.), and a more fundamental theory must be able to predict some of them.

It was realized quite some time ago that hadrons containing heavy quarks, b and c ,¹ are more tractable than the light ones. The reason is twofold: first, under favorable circumstances the large energy scale involved enables one to argue that, by virtue of asymptotic freedom, the perturbative calculation provides a reasonable first approximation. Second, new approximate symmetries arise in the limit of large quark masses, resulting in many new relations between physical quantities. Using these observations, a lot of progress in our understanding of hadrons containing a single heavy quark has been made in the last few years. One consequence of these theoretical developments was a better measurement of several Standard Model parameters, notably the heavy quark masses, and the Cabibbo-Kobayashi-Maskawa angles $|V_{cb}|$ and, to a lesser extent, $|V_{ub}|$. This work describes some of this progress, focussing on the precision measurements of the abovementioned parameters. After introducing the necessary theoretical background in Chapter 2, we discuss in Chapter 3 the model-independent determination of $|V_{cb}|$ in the exclusive semileptonic decay $B \rightarrow D^* \ell \bar{\nu}$. Chapter 4 is devoted to the inclusive B decays and their use in the measurement of $|V_{cb}|$, the heavy quark masses, and certain nonperturbative matrix elements charac-

¹The top is so heavy that it decays before hadronization takes place.

terizing the structure of the heavy mesons. In Chapter 5 we describe how the rare decay $b \rightarrow s\gamma$ can be used to measure precisely the bottom quark mass. Concluding remarks are presented in Chapter 6.

Chapter 2 Theoretical background

2.1 Heavy quark symmetry

“You boil it in sawdust: you salt it in glue:

You condense it with locusts and tape:

Still keeping one principle object in view—

To preserve its symmetrical shape.”

Lewis Carroll [1]

Consider a hadron containing a quark with a mass m_Q much bigger than the characteristic scale of strong interactions, Λ_{QCD} . It is clear that the energy and momentum of the light constituents (gluons and light quarks) will be of order Λ_{QCD} , and the velocity of the heavy quark in the rest frame of the meson will be of order $|\mathbf{v}| \sim \frac{\Lambda_{\text{QCD}}}{m_Q} \ll 1$. This means that in the first approximation the heavy quark can be treated as a static source of the chromoelectric field. Further, since the chromomagnetic moment of a quark is inversely proportional to its mass, the heavy quark spin decouples. We conclude that the light constituents of the hadron (collectively known as the “brown muck”) are sensitive to neither the mass of the quark (provided it is big enough for the static approximation to be applicable), nor the orientation of its spin. In general, when properties of a physical object are not changed by certain kinds of tampering, physicists call these allowed kinds of tampering symmetry transformations. If we have N flavors of heavy quarks, each of spin $1/2$, we can substitute one flavor of quark for another, or flip the spin of the quark, without changing the structure of the “brown muck.” This approximate symmetry is called Heavy Quark Symmetry (HQS) [3], and the corresponding transformations form a unitary group $U(2N)$. In the real world, only b and c quarks deserve to be called heavy, so HQS will be applicable only to bottom and charmed mesons and baryons.

HQS is not manifest in the QCD Lagrangian, which makes it a bit hard to use (see however Ref. [3]). To make it explicit, one has to pass to an effective field theory description of strong interactions, with all short-wavelength fluctuations capable of noticing the tampering integrated out. If we limit ourselves to systems containing one or zero heavy quarks at a time, the number of heavy quarks of each flavor in this effective theory is conserved, since producing heavy pairs requires hard quanta in the initial state. In such a theory the relation between a heavy quark Q and its antiparticle \bar{Q} is lost, and each of them is described by a separate field. In fact, since we will be dealing exclusively with systems containing just one of them, say Q , we may forget about the \bar{Q} 's from now on. The Q 's will then be described in our theory by a spinor field $h(x)$ with two independent components.

By now it should be clear that what we are trying to do is very similar to the standard Foldy-Wouthuysen transformation. In fact, at tree level (if we treat the color field as the classical background) it is *exactly* the Foldy-Wouthuysen transformation. At this level the relation between the full quark field $Q(x)$ and its effective theory relative $h(x)$ is given by well-known QED formulae [4], with electromagnetic potential and field strength replaced by their QCD counterparts. Of course the Foldy-Wouthuysen procedure breaks Lorentz invariance of the theory, but this is to be expected: after all there is a preferred frame in this problem, the rest frame of the heavy meson. Still, it is convenient to preserve at least Lorentz *covariance* by letting the preferred rest frame have an arbitrary 4-velocity v . Then the heavy quark will be described by a v -dependent Dirac spinor $h_v(x)$ satisfying

$$\frac{1 + \not{v}}{2} h_v(x) = h_v(x). \quad (2.1)$$

This constraint ensures that the field $h_v(x)$ has only two independent components, which describe the two spin states of the heavy quark. In the rest frame of the meson, where $v = (1, \mathbf{0})$, Eq. (2.1) reduces to the requirement that the two lower components of h_v be zero. ‘‘Covariantizing’’ the standard formulae from Ref. [4], we arrive at the following relation between $Q(x)$ and $h_v(x)$:

$$Q(x) = e^{-im_Q v \cdot x} \left(1 + \frac{i\not{D}_\perp}{2m_Q} + \frac{(v \cdot D)\not{D}_\perp}{4m_Q^2} - \frac{\not{D}_\perp^2}{8m_Q^2} + \mathcal{O}\left(\frac{1}{m_Q^3}\right) \right) h_v(x), \quad (2.2)$$

where $D_\mu = \partial_\mu - igA_\mu$ is the covariant derivative, and $D_\perp = D - v(v \cdot D)$. Similarly, we can easily read off the tree level Lagrangian for h_v from Ref. [4]:

$$\begin{aligned} \mathcal{L} &= \bar{h}_v i v \cdot D h_v + \frac{1}{2m_Q} \bar{h}_v (iD_\perp)^2 h_v + \frac{1}{2m_Q} \bar{h}_v \frac{g}{2} \sigma_{\mu\nu} G^{\mu\nu} h_v \\ &\quad - \frac{1}{4m_Q^2} \bar{h}_v i\not{D}_\perp (i v \cdot D) i\not{D}_\perp h_v + \frac{1}{8m_Q^2} \bar{h}_v (i\not{D}_\perp)^2 (i v \cdot D) h_v \\ &\quad + \frac{1}{8m_Q^2} \bar{h}_v (i v \cdot D) (i\not{D}_\perp)^2 h_v + \mathcal{O}\left(\frac{1}{m_Q^3}\right). \end{aligned} \quad (2.3)$$

Beyond tree level, the Lagrangian of the Heavy Quark Effective Theory (HQET) must be constructed as the most general linear combination of local operators built out of $h_v(x)$ and other fields which is consistent with the symmetries of QCD. The coefficients in this Lagrangian are determined by matching amplitudes in HQET and full QCD order by order in α_s . The higher the dimension of the operator, the more its coefficient is suppressed by powers of m_Q . Therefore only a few operators will be relevant in practice. Actually, there is an ambiguity in this construction related to the freedom to redefine the heavy field $h_v(x)$. To eliminate this ambiguity, we will require that $h_v(x)$ and $h_v^\dagger(x)$ have canonical commutation relations.¹ This ensures that at tree level the part of the effective Lagrangian depending on h_v is identical to the Lagrangian obtained by the Foldy-Wouthuysen procedure, Eq. (2.3). The leading (dimension-four) contribution to the HQET Lagrangian has the following form [5]:

$$\mathcal{L}_{HQET} = \bar{h}_v i v \cdot D h_v + \mathcal{L}_{light}, \quad (2.4)$$

where \mathcal{L}_{light} is the standard QCD Lagrangian for gluons and light quarks. (One could think that there is a candidate operator of dimension three as well, namely $\bar{h}_v h_v$. However its coefficient can always be made zero by redefining the heavy field

¹Though very natural, this is by no means a standard choice.

according to $h_v(x) \rightarrow e^{ia v \cdot x} h_v(x)$ with some a .) Since we required that h_v and h_v^\dagger were canonically conjugate variables, higher-dimensional contributions to the HQET Lagrangian will not contain the “time derivative” $v \cdot D$ acting on h_v .

The Lagrangian Eq. (2.4) has manifest HQS: it does not care about either spin or flavor of the heavy quark. Higher dimensional contributions will break this symmetry. The corrections due to operators of dimension five are

$$\Delta\mathcal{L}_5 = \frac{C_{kin}}{2m_Q} \bar{h}_v (iD_\perp)^2 h_v + \frac{C_{mag}}{2m_Q} \bar{h}_v \frac{g}{2} \sigma_{\mu\nu} G^{\mu\nu} h_v. \quad (2.5)$$

In Eq. (2.5) only the operators which depend on $h_v(x)$ are included.²

The coefficients in Eq. (2.5) are determined by matching amplitudes in HQET and full QCD order by order in perturbation theory. Thus we are making a double expansion in α_s and $1/m_Q$. Beyond tree level matching requires choosing a renormalization scheme. Physically, the most transparent renormalization procedure would be to cut off the loop integrals in HQET at some scale Λ . This is the Wilsonian renormalization group approach. Technically, it is much more convenient to use dimensional regularization and the $\overline{\text{MS}}$ subtraction scheme both for HQET and full QCD diagrams, with the subtraction point μ replacing the ultraviolet cutoff Λ . This is what we are going to do in what follows.³

Both C_{kin} and C_{mag} are 1 at the tree level. It can be shown that $C_{kin} = 1$ to all orders in α_s [6]. The coefficient C_{mag} has been computed to order α_s , and leading logarithms of the form $\alpha_s^n \log^n \frac{\mu}{m_Q}$ have been summed up [7]. The result is

$$C_{mag}(\mu) = \left(\frac{\alpha_s(m_Q)}{\alpha_s(\mu)} \right)^{3/\beta_0} \left(1 + \frac{13}{6} \frac{\alpha_s}{\pi} \right), \quad (2.6)$$

where $\beta_0 = 11 - 2n_f/3$.

The contribution from dimension-six operators being suppressed by extra power

²To be precise, we must specify what m_Q means. For us, m_Q will always denote the quark pole mass.

³The admissibility of dimensional regularization in HQET was a subject of some debate. Our point of view on this is expounded in Section 2.3.

of m_Q relative to Eq. (2.5), we will need it only at the tree level. The corresponding expression can be read off Eq. (2.3):

$$\begin{aligned} \Delta\mathcal{L}_6 &= -\frac{1}{4m_Q^2}\bar{h}_v i\not{D}_\perp (iv \cdot D) i\not{D}_\perp h_v + \frac{1}{8m_Q^2}\bar{h}_v (i\not{D}_\perp)^2 (iv \cdot D) h_v \\ &+ \frac{1}{8m_Q^2}\bar{h}_v (iv \cdot D)(i\not{D}_\perp)^2 h_v. \end{aligned} \quad (2.7)$$

Although Eq. (2.7) seems to contain the time derivatives of h_v , it can be rewritten in a form in which only spatial derivatives show up. This is a consequence of how the Foldy-Wouthuysen transformation is constructed.

Let us apply this formalism to the spectroscopy of heavy mesons. By virtue of HQS, the spin of the heavy quark is conserved, and therefore the total angular momentum of the “brown muck” is conserved too. Thus we can label the heavy meson states by their parity P , total spin j , and the spin of the light degrees of freedom s_ℓ . The heavy quark spin being $1/2$, for fixed s_ℓ the total spin can take values $j = s_\ell \pm \frac{1}{2}$. HQS implies that these two states are degenerate. Thus heavy mesons come in doublets labeled by s_ℓ^P . This is what is observed in nature – see Table 2.1.⁴ HQS also predicts that the splitting between the $\frac{1}{2}^-$ and $\frac{3}{2}^+$ doublets is the same for charmed and bottom mesons. This also seems to be true, if all the resonances with undetermined quantum numbers are interpreted as what their names suggest.

To understand the deviations from the HQS predictions, let us derive the meson mass formulae to order $\Lambda_{\text{QCD}}^3/m_Q^2$ [9, 10, 11]. (We will use these formulae extensively in the following chapters.)

First let us introduce some notation. Let $|H(v)\rangle$ be the state representing a heavy meson with 4-velocity $v = (1, \mathbf{0})$. It is an eigenstate of the full QCD Hamiltonian with the eigenvalue m_H . Let \mathcal{H}_{HQET} be the Hamiltonian corresponding to the Lagrangian Eq. (2.4), and $\mathcal{H} = \mathcal{H}_{HQET} + \Delta\mathcal{H}$ be the Hamiltonian derived from the Lagrangian $\mathcal{L}_{HQET} + \Delta\mathcal{L}$, where $\Delta\mathcal{L} = \Delta\mathcal{L}_5 + \Delta\mathcal{L}_6 + \dots$ represents corrections from operators of

⁴The table includes all known heavy meson resonances, including those which did not even make it to the PDG Summary Table [8].

	Name	$I(J^P)$	Mass, GeV	s_ℓ^P
Charm	D	$1/2(0^-)$	1.87	$1/2^-$
	D*	$1/2(1^-)$	2.01	$1/2^-$
	D ₁	$1/2(1^+)$	2.42	$3/2^+$
	D ₂ *	$1/2(2^+)$	2.46	$3/2^+$
	D _s	$0(0^-)$	1.97	$1/2^-$
	D _s *	$?(?)$	2.11	$1/2^-$
	D _{s1} (2536)	$0(1^+)$	2.54	$3/2^+$
	D _{sJ} (2573)	$?(?)$	2.57	$3/2^+$
	Bottom	B	$1/2(0^-)$	5.28
B*		$1/2(1^-)$	5.32	$1/2^-$
B _J *(5732)		$?(?)$	5.73	$3/2^+$
B _s		$0(0^-)$	5.37	$1/2^-$
B _s *		$?(?)$	5.42	$1/2^-$
B _{sJ} *(5850)		$?(?)$	5.85	$3/2^+$

Table 2.1: Observed heavy mesons and their assignment to HQS doublets.

dimension five and higher. By construction, $\Delta\mathcal{L}$ does not contain time derivatives, therefore $\Delta\mathcal{H} = -\Delta\mathcal{L}$. The effective theory Hamiltonian \mathcal{H} being equivalent to the full QCD Hamiltonian, $|H(v)\rangle$ is an eigenstate of \mathcal{H} . The corresponding eigenvalue is $m_H - m_Q$, since in the effective theory the energy is counted from the rest mass of the heavy quark. Finally let us denote by $|H_\infty(v)\rangle$ the limit of $|H(v)\rangle$ as $m_Q \rightarrow \infty$. Evidently, this limit exists and is the eigenstate of \mathcal{H}_{HQET} . We denote the corresponding eigenvalue by $\bar{\Lambda}$.

Our starting point is the identity

$$m_H = m_Q + \left[\frac{1}{2} \frac{\langle H_\infty(v) | \mathcal{H} | H(v) \rangle}{\langle H_\infty(v) | H(v) \rangle} + h.c. \right]. \quad (2.8)$$

Using the definitions of \mathcal{H} and $|H_\infty(v)\rangle$, and the Gell-Mann and Low theorem (see, e.g., Ref. [12]), Eq. (2.8) can be manipulated into the following form:

$$m_H = m_Q + \bar{\Lambda} - \frac{1}{2} \left[\frac{\langle H_\infty(v) | \Delta\mathcal{L} T \exp \left(i \int d^3x \int_{-\infty}^0 dt \Delta\mathcal{L}(x) \right) | H_\infty(v) \rangle}{\langle H_\infty(v) | T \exp \left(i \int d^3x \int_{-\infty}^0 dt \Delta\mathcal{L}(x) \right) | H_\infty(v) \rangle} + h.c. \right]. \quad (2.9)$$

Expanding Eq. (2.9) up to terms of relative order $1/m_b^3$ we obtain the mass formula:

$$m_H = m_Q + \bar{\Lambda} - \langle H_\infty(v) | \Delta\mathcal{L}_5 + \Delta\mathcal{L}_6 | H_\infty(v) \rangle \quad (2.10)$$

$$- \left[\frac{1}{2} \langle H_\infty(v) | \Delta\mathcal{L}_5(0) i \int d^3x \int_{-\infty}^0 dt \Delta\mathcal{L}_5(x) | H_\infty(v) \rangle + h.c. \right].$$

$\Delta\mathcal{L}_5$ and $\Delta\mathcal{L}_6$ are given by Eq. (2.5) and Eq. (2.7) respectively. We normalize one-particle states to 1 per unit volume here and in what follows.

Eq. (2.10) contains expectation values of both local and nonlocal operators. When H is the ground-state ($s_\ell^P = \frac{1}{2}^-$) doublet, it is convenient to introduce a shorthand notation for these expectation values:

$$\lambda_1 = \langle H_\infty(v) | \bar{h}_v (iD_\perp)^2 h_v | H_\infty(v) \rangle, \quad (2.11)$$

$$\lambda_2 = \frac{1}{d_H} \langle H_\infty(v) | \bar{h}_v \frac{g}{2} \sigma_{\mu\nu} G^{\mu\nu} h_v | H_\infty(v) \rangle,$$

$$\langle H_\infty(v) | \bar{h}_v (iD_\alpha) (iD_\mu) (iD_\beta) h_v | H_\infty(v) \rangle = \frac{1}{3} \rho_1 (g_{\alpha\beta} - v_\alpha v_\beta) v_\mu, \quad (2.12)$$

$$\langle H_\infty(v) | \bar{h}_v (iD_\alpha) (iD_\mu) (iD_\beta) \gamma_\delta \gamma_5 h_v | H_\infty(v) \rangle = \frac{1}{6} d_H \rho_2 i \epsilon_{\nu\alpha\beta\delta} v^\nu v_\mu,$$

$$\langle H_\infty(v) | \bar{h}_v (iD_\perp)^2 h_v i \int d^3x \int_{-\infty}^0 dt \Delta\mathcal{L}_5(x) | H_\infty(v) \rangle + h.c. = \frac{\mathcal{T}_1 + d_H \mathcal{T}_2}{m_Q}, \quad (2.13)$$

$$\langle H_\infty(v) | \bar{h}_v \frac{g}{2} \sigma_{\mu\nu} G^{\mu\nu} h_v i \int d^3x \int_{-\infty}^0 dt \Delta\mathcal{L}_5(x) | H_\infty(v) \rangle + h.c. = \frac{\mathcal{T}_3 + d_H \mathcal{T}_4}{m_Q},$$

where $d_H = 3$ or -1 depending on whether H_∞ is a pseudoscalar or a vector. In terms of these matrix elements the meson mass is given by

$$m_H = m_b + \bar{\Lambda} - \frac{\lambda_1 + d_H C_{mag} \lambda_2}{2m_Q} + \frac{\rho_1 + d_H \rho_2}{4m_Q^2} - \frac{\mathcal{T}_1 + \mathcal{T}_3 + d_H(\mathcal{T}_2 + \mathcal{T}_4)}{4m_Q^2}. \quad (2.14)$$

In particular, the leading order deviations from HQS are described just by two matrix elements of local dimension-five operators, λ_1 and λ_2 . Dimensional analysis suggests that they are both of order Λ_{QCD}^2 . We will see in the next section that the leading nonperturbative corrections to the semileptonic decay rates of B mesons are described

by the same two matrix elements, so it is important to know their numerical values. According to Eq. (2.14), $C_{mag}(\mu)\lambda_2(\mu)$ determines the splitting between the members of the ground-state doublet. Therefore, if one neglects the corrections of order $\Lambda_{\text{QCD}}^3/m_b^2$, one can use the measured splitting between B and B^* mesons to extract the value $C_{mag}(\mu)\lambda_2(\mu) \simeq 0.12 \text{ GeV}^2$.⁵ It is much harder to determine λ_1 . In Chapter 4 we show how one can extract λ_1 and $\bar{\Lambda}$ from the measured charged lepton spectrum in the inclusive semileptonic B decay.

In the following chapters we will often need the values of the quark masses m_b and m_c to make numerical estimates. According to Eq. (2.14) the difference $m_b - m_c$ is given by

$$m_b - m_c = \bar{m}_B - \bar{m}_D - \lambda_1 \left(\frac{1}{2\bar{m}_D} - \frac{1}{2\bar{m}_B} \right) + \mathcal{O} \left(\frac{\Lambda_{\text{QCD}}^3}{\bar{m}_D^2} \right), \quad (2.15)$$

where $\bar{m}_B = (m_B + 3m_{B^*})/4$, $\bar{m}_D = (m_D + 3m_{D^*})/4$. QCD sum rule estimates of λ_1 range from -0.1 GeV^2 to -0.6 GeV^2 [13, 14]. Roughly the same range results from the analysis of Chapter 4. Thus we take $\lambda_1 = -0.3 \pm 0.3 \text{ GeV}^2$. As for the error from terms of order $\Lambda_{\text{QCD}}^3/\bar{m}_D^2$, we conservatively estimate it as $(0.5 \text{ GeV})^3/\bar{m}_D^2 \simeq 0.03 \text{ GeV}$. Then Eq. (2.15) implies $m_b - m_c = 3.39 \pm 0.08 \text{ GeV}$. To determine m_b and m_c separately, one needs to know $\bar{\Lambda}$. QCD sum rules give $\bar{\Lambda} = 0.5 \pm 0.1 \text{ GeV}$ [13]. This value for $\bar{\Lambda}$ is consistent with the results of Chapter 4, although the latter have much larger uncertainty. According to Eq. (2.14) $\bar{m}_B = m_b + \bar{\Lambda} + \mathcal{O}(\Lambda_{\text{QCD}}^2/m_b)$, so using $\bar{\Lambda} = 0.5 \pm 0.1 \text{ GeV}$ we obtain $m_b = 4.8 \pm 0.1 \text{ GeV}$. On the other hand, estimates of m_b based on sum rules for bottomonium give contradicting results [15], but in general produce values in the range $4.55 - 4.8 \text{ GeV}$. To be conservative, we adopt $m_b = 4.8 \pm 0.2 \text{ GeV}$. Then $m_c = 1.41 \pm 0.28 \text{ GeV}$.

We would like to conclude this section with a lightning review of the use of HQET in the study of exclusive weak decays. HQET is particularly useful when applied to semileptonic and radiative decays of heavy hadrons. Here one must distinguish between heavy-to-light and heavy-to-heavy decays. HQS relates various amplitudes

⁵Both C_{mag} and λ_2 depend on the subtraction point μ , but their product does not.

in each class. For example, it relates the form factors describing $D \rightarrow \rho$ and $D \rightarrow K^*$ transitions to those describing $B \rightarrow \rho$ and $B \rightarrow K^*$ transitions respectively. This can be used, in principle, to accurately measure $|V_{ub}|$ [16]. Here we will focus on heavy-to-heavy decays. Since in real life the only heavy quarks are b and c quarks, we will sacrifice “generality” to the transparency of notation, and discuss the matrix elements of flavor-changing b -to- c currents between $B^{(*)}$ and $D^{(*)}$. This is a particularly interesting situation, since $B^{(*)}$ and $D^{(*)}$ belong to the same HQS multiplet. Consider the matrix element

$$\langle D^{(*)}(v') | J_\Gamma | B^{(*)}(v) \rangle, \quad (2.16)$$

where $J_\Gamma = \bar{c} \Gamma b$, and Γ is either γ_μ or $\gamma_\mu \gamma_5$. The differential rate of the semileptonic decay $B^{(*)} \rightarrow D^{(*)} \ell \bar{\nu}$ can be expressed through these matrix elements. The first step is to find the HQET operator corresponding to the full theory operator J_Γ . This “matching” should be done order by order in perturbation theory. At tree level, we can use Eq. (2.2) to express the heavy quark fields $c(x)$ and $b(x)$ in terms of the HQET fields $h_v^c(x)$ and $h_v^b(x)$. Then the operator J_Γ becomes

$$J_\Gamma = \bar{h}_{v'}^c(x) \left(\Gamma - \frac{i \overleftarrow{\not{D}_\perp}}{2m_c} \Gamma + \Gamma \frac{i \overrightarrow{\not{D}_\perp}}{2m_b} + \dots \right) h_v^b(x). \quad (2.17)$$

Beyond tree level, one should allow for all possible operators with the correct quantum numbers to appear on the right-hand-side of Eq. (2.17). Their coefficients are determined by the requirement that the matrix elements of the current in the full theory and in the effective theory agree to all orders in α_s and $1/m_{c,b}$. For example, neglecting all corrections of order $1/m_{c,b}$, one expects to find for the vector and axial currents

$$\begin{aligned} J_V &= \sum_{i=1}^3 C_V^{(i)}(v \cdot v', \mu) \bar{h}_{v'}^c \Gamma_i h_v^b, \\ J_A &= \sum_{i=1}^3 C_A^{(i)}(v \cdot v', \mu) \bar{h}_{v'}^c \Gamma_i \gamma_5 h_v^b, \end{aligned} \quad (2.18)$$

where

$$\Gamma_1 = \gamma^\mu, \quad \Gamma_2 = v^\mu, \quad \Gamma_3 = v'^\mu. \quad (2.19)$$

The peculiarity of HQET is that the matching coefficients $C^{(i)}$ depend on $v \cdot v'$. Because of this, even the one-loop expressions are fairly complicated [17].

Neglecting the $1/m_Q$ corrections both to the currents and to the meson states, and keeping in mind Eqs. (2.18), we are led to consider

$$\langle D_\infty^{(*)}(v') | \bar{h}_v^c \Gamma h_v^b | B_\infty^{(*)}(v) \rangle. \quad (2.20)$$

Here $|D_\infty^{(*)}\rangle$ and $|B_\infty^{(*)}\rangle$ are the states in the infinite mass limit, and therefore are just tensor products of the heavy quark spin state and the “brown muck” state. Noticing that the current acts only on the heavy quark degrees of freedom, we infer that the matrix element Eq. (2.20) is given by

$$-\xi(v \cdot v', \mu) \text{Tr}[\bar{M}(v') \Gamma M(v)], \quad (2.21)$$

where $\xi(v \cdot v', \mu)$ is a universal form factor, and $M(v)$ is the projector on the appropriate state of the HQS doublet. Using the nonrelativistic normalization of states (one particle per unit volume), these projectors can be computed to be

$$M(v) = \frac{1 + \not{v}}{2\sqrt{2}} \begin{cases} -\gamma_5 & \text{for the pseudoscalar} \\ \not{v} & \text{for the vector} \end{cases}. \quad (2.22)$$

Thus, if one neglects the $1/m_Q$ corrections, all the form factors are expressed through a single function ξ , known as the Isgur-Wise function.

The Isgur-Wise function cannot be computed perturbatively. However, its value at zero recoil ($v \cdot v' = 1$) is fixed by HQS to be 1. To see this, consider the matrix element of the flavor-conserving current $\bar{h}_v^b \gamma_\mu h_v^b$ between the B-meson states $|B_\infty\rangle$ with the same velocity. By HQS, it is given by Eq. (2.21) with $v = v'$. A short computation shows that the matrix element in question is just given by $\xi(1)v_\mu$. On the other hand, this current is conserved, and furthermore the B-meson state is the

eigenstate of the corresponding charge with eigenvalue 1. This proves that $\xi(1) = 1$. In the next chapter we will see how this fact can be used to accurately measure $|V_{cb}|$ in the exclusive decay $B \rightarrow D^* \ell \bar{\nu}$.

2.2 Heavy quark expansion

Since the mid seventies, inclusive weak decays of heavy hadrons were described using the parton model. In other words, in order to predict the rate and the spectrum of final states in a certain inclusive decay, one just computed the corresponding quantities for the free heavy quark decay. The justification for such a procedure was that these decays occur on a short time scale, the energy release being large. Therefore one could argue that the total probability for a heavy quark to decay does not depend on the “brown muck.” The situation with final state spectra was less clear, but it was known that the lepton spectrum in the inclusive B and D decays agrees with the parton model predictions quite well. An *ad hoc* model of Altarelli *et al.*, [18] which attempted to incorporate the effect of the heavy quark “Fermi motion,” led to the same conclusion. However, the limits of the parton model description remained unclear. Only relatively recently was it realized [19] that in many cases one can justify the parton model, and even compute corrections to its predictions, using the Operator Product Expansion (OPE) and some additional qualitative assumptions collectively known as quark-hadron duality.

The basic idea of Ref. [19] is simple enough. Suppose we are interested in an inclusive weak decay of a heavy hadron H which is mediated by a quark bilinear $J_\Gamma = \bar{q} \Gamma Q$. Here Q is the initial heavy quark, and q is the final state quark which may or may not be heavy. Consider the expectation value of the time-ordered product

$$T(q^2, q \cdot v) = -i \int d^4 x e^{-iq \cdot x} \langle H(v) | T [J_\Gamma^\dagger(x) J_\Gamma(0)] | H(v) \rangle. \quad (2.23)$$

The current J_Γ has some Lorentz indices, and therefore in general T is a tensor, but

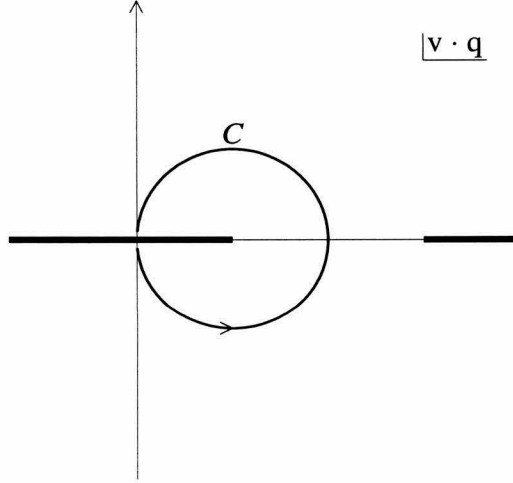


Figure 2.1: The analytic structure of the time-ordered product of two heavy quark currents.

this need not concern us here. Let us also define

$$W(q^2, q \cdot v) = (2\pi)^3 \sum_X \delta^4(p_H - q - p_X) \langle H(v) | J^\dagger | X \rangle \langle X | J | H(v) \rangle. \quad (2.24)$$

The differential decay rate can be expressed in terms of W . It is easy to see that $W = -\frac{1}{\pi} \text{Im}T$. It is convenient to regard T as a function of complex variables q^2 and $q \cdot v$. The analytic structure of T at fixed real q^2 in general looks like Fig. 2.1. The two cuts correspond to two possible time orderings of the currents in Eq. (2.23). Only the ordering giving the left cut corresponds to the decay process, the other cut corresponding to the states containing two Q 's. W may be regarded as a discontinuity of T across the physical cut.

Of course, computing T for all q^2 and $q \cdot v$ is beyond our capabilities. However, far away from the cuts T can be computed using the OPE, since in this situation all intermediate states are highly virtual. More concretely, the time-ordered product of currents always admits a short distance expansion of the form

$$T [J_\Gamma^\dagger(x) J_\Gamma(0)] \underset{x \rightarrow 0}{\sim} \sum_{\mathcal{O}} C_{\mathcal{O}}(x) \mathcal{O}(0), \quad (2.25)$$

where \mathcal{O} are local operators, and $C_{\mathcal{O}}$ are c -number coefficients. If q is chosen so that all physical intermediate states are far off-shell, then we expect that the Fourier transform of Eq. (2.25) will be dominated by several operators of lowest dimension, whose coefficients can be computed in perturbation theory.

How can we use our knowledge of T in the unphysical region of the $q \cdot v$ plane? Suppose we would like to compute the inclusive differential rate $d\Gamma/dq^2$. It is given by an integral of W with an appropriate weight along the physical cut. The lower limit of the integral depends of the nature of the process, but the upper limit is always the end of the physical cut. This integral can be interpreted as an integral of T along the contour shown in Fig. 2.1. The integrand can be computed everywhere on the contour except where it touches the cut. Neglecting this problem for the time being, we may conclude that $d\Gamma/dq^2$ is calculable by means of the OPE. Similarly, one can argue that other inclusive observables are calculable.

The problem is simplified further by the observation that one may keep track only of those operators whose expectation values in the initial hadron state are nonzero, and only if the Fourier transform of their coefficients has a discontinuity across the cut in the physical region. For example, at leading order in α_s , the coefficient of the unit operator is given by the diagram in Fig. 2a, while the coefficients of all operators of the form $\bar{Q}\Gamma_A Q$ can be extracted from the diagram in Fig. 2b. But it is easy to see that the diagram in Fig. 2a has no imaginary part for values of q relevant for the decay process in question, and therefore the unit operator may be omitted.

Typically, the relevant operators are of the form $\bar{Q}D_{\mu_1} \dots D_{\mu_n} Q$ (we omitted the Dirac structure). To argue that only a few operators of lowest dimension are important, one has to show that derivatives scale like Λ_{QCD} . In fact, this statement is just plain wrong if Q is the ordinary quark field, since the time-like component of the heavy quark momentum is very nearly m_Q . However, it is rather obvious how to circumvent this problem: one has to perform the OPE in terms of the “rescaled” field $Q_{eff}(x) = e^{im_Q v \cdot x} Q(x)$ rather than in terms of $Q(x)$. Then the derivatives will bring down powers of the residual momentum of the quark, i.e., the quark momentum with

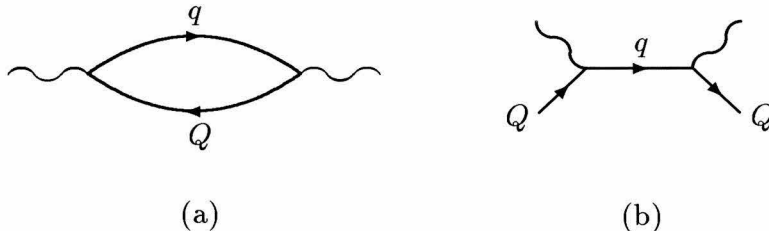


Figure 2.2: Diagrams representing the OPE coefficients at the tree level. The coefficient of the unit operator is given by diagram (a). The coefficients of the heavy quark bilinears $\bar{Q}\Gamma_A Q$ can be determined from diagram (b). Wavy lines denote the insertions of the current $\bar{q}\Gamma Q$.

$m_Q v$ subtracted, which is indeed of order Λ_{QCD} .⁶ Recall that the relation between $Q(x)$ and the HQET field, Eq. (2.2), involved the same factor $e^{im_Q v \cdot x}$. Thus it is natural (though not absolutely necessary) to go one step further and to do the OPE in terms of the HQET field $h_v(x)$. The advantage is threefold. First, $h_v(x)$ satisfies the constraint Eq. (2.1), which makes the Dirac algebra simpler. Second, counting powers of m_Q is more straightforward in HQET than in full QCD. Third, the number of nonperturbative matrix elements parametrizing the decay rate can be reduced by taking into account the requirements of HQS. In the effective theory this is very easy to do, since HQS is manifest.

For example, for semileptonic B -decay the leading (dimension three) operator in the OPE is $\bar{Q}\gamma_\mu Q$, the conserved current, and its expectation value is just v_μ . It is not necessary to pass to the effective theory to evaluate it. The contribution of this operator to the differential decay rate is exactly the parton model result. The only dimension four operator is $\bar{h}_v D_\mu h_v$. Using the equations of motion of HQET, its expectation value in the B -meson state can be expressed in terms of the expectation values of dimension five operators [20]. Because of this, the corrections to the parton model result are suppressed by two powers of m_Q . They are parametrized by the matrix elements of two dimension five operators: the kinetic energy operator $\bar{h}_v (iD_\perp)^2 h_v$, and the chromomagnetic operator $\bar{h}_v \sigma \cdot G h_v$. Their expectation values are just λ_1 and λ_2 defined in Eq. (2.11).

⁶In retrospect, it seems surprising that it took more than a decade to realize this.

Naturally, there are limitations to this approach. The OPE works only if the intermediate states are far off-shell. For this to hold everywhere on the contour in Fig. 2.1, the distance between the cuts must be of order 1 GeV or more. In $b \rightarrow c$ decays the cuts are always separated by at least $2m_c$, and over most of the phase space the distance is of order m_b . These are large enough scales for the OPE to be applicable. On the other hand, in $b \rightarrow u$ decays the cuts merge when q^2 is maximal, i.e., when the leptons are back-to-back. Thus the OPE fails in one corner of the Dalitz plot.

It remains to discuss what to do with the parts of the contour in Fig. 2.1 which lie near the cut. Here the notion of quark-hadron duality [21] comes in handy. Notice that the expression for T as given by the OPE has analytic structure similar to Fig. 2.1, except that the positions of the cuts are determined by the heavy quark mass m_Q rather than by the hadron mass m_H . One can think of the OPE as computing the decay rate in terms of quark and gluon degrees of freedom, although the actual final state consists of hadrons. In fact, the leading term in the OPE is always the same as the parton model result. Of course, we cannot expect the parton model to exactly reproduce W , since the latter may receive contributions from hadronic resonances which are absent in perturbation theory. However, if the hadronic invariant mass is large, the resonances must be very broad and overlap significantly. In this case we do expect perturbation theory to reproduce W accurately. This is the postulate of local quark-hadron duality [21]. It seems very reasonable from the physical point of view and has numerous experimental confirmations, e.g., in e^+e^- annihilation. A less stringent assumption is that the OPE reproduces W smeared over an interval of hadronic masses of order Λ_{QCD} . We will refer to this as global quark-hadron duality.

The upshot of the above discussion is that if the contour approaches the cut where the hadronic invariant mass is allowed to be large, we can justify using the expression for T obtained from the OPE. This is the situation for the total semileptonic decay rate $B \rightarrow X_c \ell \bar{\nu}$. Moreover, the above argument shows that the lepton spectrum is also computable using the OPE provided we do not come too close to the end point. For only a few hadronic states are kinematically allowed if the lepton energy

is close to the maximum. Similarly, global quark-hadron duality tells us that we can compute the properties of the averaged hadron spectrum. If we were bold enough to trust local duality, we could also compute the hadron spectrum point by point for the region where the hadronic mass is large.

In principle, the ability to predict the inclusive semileptonic B width enables one to measure precisely the mixing angle $|V_{cb}|$. The difficulty is that the prediction also contains the quark pole masses m_b and m_c which are not well known. The mass formulae of Section 2.1 can be used to express m_b and m_c in terms of well known meson masses and various nonperturbative matrix elements. If we neglect dimension-six operators, we are left with only with three of them: $\bar{\Lambda}$, λ_1 and λ_2 . As mentioned previously, the value of λ_2 is known, while the values of the other two are not. One possibility is to try to determine $\bar{\Lambda}$ and λ_1 using QCD sum rules [13, 14]. Another is based on the observation that these same two quantities influence the shape of the lepton spectrum in the decay $B \rightarrow X_c \ell \bar{\nu}$, and therefore can be extracted from experiment. This possibility is explored in Chapter 4. Still another way to measure $\bar{\Lambda}$ and λ_1 (in the decay $B \rightarrow X_s \gamma$) is discussed in Chapter 5.

2.3 Renormalons as a red herring

To compute OPE coefficients beyond tree level one has to choose a regularization procedure. Usually, dimensional regularization is the most convenient method because it maintains gauge invariance and automatically subtracts power divergences. But often it is argued that, unlike a sharp momentum cutoff, dimensional regularization does not achieve the strict separation of scales. If this were true, one would be forced to abandon dimensional regularization, since separation of short- and long-distance physics is the very idea of the OPE. However, the abovementioned arguments are not entirely convincing.

At any finite order of perturbation theory there does not seem to be a problem. Consider for simplicity an OPE for an observable depending on a single momentum

scale Q :

$$A(Q) = C_0(Q) + \frac{C_2(Q)}{Q^2} \langle O_2(Q) \rangle + \frac{C_4(Q)}{Q^4} \langle O_4(Q) \rangle + \dots \quad (2.26)$$

Here C_i are perturbatively calculable coefficients, and O_i are operators of dimension i . One could regard Eq. (2.26) as a way to present $A(Q)$ so that the power-like dependence on Q is made explicit. The logarithmic dependence is buried in C_i and O_i . The coefficients C_i can be computed in perturbation theory, while for matrix elements $\langle O_i \rangle$ only the Q dependence can be determined.

The difficulties start when one tries to give the expansion in Eq. (2.26) a meaning beyond perturbation theory. Apriori, it is not clear that the series defining the coefficients C_i are convergent. In fact, there are reasons to believe that they are only asymptotic [22]. One popular approach to this problem is to define the sum of an asymptotic series using the Borel prescription. Let us consider a series

$$S(x) = a_0 + a_1 x + a_2 x^2 + \dots + a_n x^n + \dots \quad (2.27)$$

The idea behind the Borel prescription is to consider an associated series

$$S_B(t) = a_1 + a_2 t + \frac{a_3}{2} t^2 \dots + \frac{a_{n+1}}{n!} t^n + \dots \quad (2.28)$$

Suppose this new series converges and defines an analytic function for all nonnegative t . Then the sum of the series Eq. (2.27) is naturally defined as

$$a_0 + \int_0^\infty S_B(t) e^{-t/x} dt. \quad (2.29)$$

It is easy to check that the expansion of the integral Eq. (2.29) in powers of x reproduces Eq. (2.27). The problem arises if $S_B(t)$ has poles on the positive real axis. Then the integral in Eq. (2.29) is not well-defined, and the Borel prescription is ambiguous. These ambiguities are called renormalons.

It is often said that if the OPE has a meaning beyond perturbation theory, then the series defining C_i must be free of renormalons, i.e., Borel-summable. Obviously, one

would prefer to have converging series, but, lacking convergence, Borel-summability is argued to be the next best thing. Our first objection is that Borel prescription is *ad hoc*: there are other ways to define a sum for an asymptotic series (see, e.g., Ref. [23]). Further, it is stated that dimensional regularization yields series which contain renormalons, and therefore is deficient. Let us inspect this argument more closely. It is extremely difficult to establish the large-order behaviour of perturbation theory. No rigorous results (even at a physical level of rigour) have been obtained for $D = 4$ field theories. Instead, the argument is based on the large-order behaviour of a small gauge-invariant subclass of Feynman diagrams. They are obtained from the tree diagrams by insertion of a chain of one-loop vacuum polarization diagrams into the gluon propagators. Technically, the summation of these contributions amounts to replacing $\alpha_s(\mu)$ by $\alpha_s(k)$, where k is the momentum flowing through the propagator. Since $\alpha_s(k)$ has a pole at $k = \Lambda_{\text{QCD}}$, the result is ambiguous. This is how renormalon ambiguity manifests itself here. Therefore, the argument goes, the dimensionally regularized C_i pick up unwanted and ambiguous infrared contributions which in all honesty should reside in $\langle O_i \rangle$. In other words, there are ambiguities in both C_i and $\langle O_i \rangle$, and only their product is well defined. However, if one imposes a sharp infrared cutoff at $k = \Delta > \Lambda_{\text{QCD}}$, the result is well defined, and there are no renormalons in C_i . An obvious flaw in such reasoning is that it relies on the summation of a small subclass of diagrams. This subclass does not dominate in any reasonable limit of QCD, and thus the actual behaviour of the perturbation theory may be quite different. In particular, there is no guarantee that imposing a sharp cutoff makes the series Borel summable.

From the practical point of view, the issue of renormalons is irrelevant. After all, we can compute only a couple of terms in perturbation theory, and what happens at large orders is of purely academic interest. The relevant question is what is the meaning of the matrix elements $\langle O_i \rangle$ in the absence of a nonperturbative definition of the OPE. The answer is that one should regard them as uncalculable parameters which must be determined by fitting Eq. (2.26) to experimental data. Once the $\langle O_i \rangle$ are measured their values can be used to predict other observables. One may

be worried that since the coefficients C_i are known only to a finite order in $\alpha_s(Q)$, neglecting higher orders in perturbation theory may introduce large uncertainties in the extracted values of the “condensates” $\langle O_i \rangle$. Indeed, at sufficiently large Q the neglected terms in C_0 are always larger than the condensate contributions, since the former are suppressed by powers of $\log Q^2$ while the latter are suppressed by at least Q^2 . The resolution is that the extraction of condensates by fitting $A(Q)$ is possible only if there is a range of Q in which the neglected terms in C_0 are small, while the condensate contribution is still important. The existence of such a range can be settled only on a case-by-case basis [24]. Similarly, the measured values of the condensates can be used to improve predictions for other observables only if the neglected perturbative corrections are small compared to the condensate contributions. Otherwise perturbative uncertainties dominate, and one gains nothing by including nonperturbative effects.

Similar issues are involved when one tries to extract $\langle O_i \rangle$ from lattice Monte-Carlo simulations. In fact, one may regard such simulations as some kind of “experiment,” the role of C_i being taken by matching coefficients between the lattice and continuum.

Chapter 3 The decay $B \rightarrow D^* \ell \bar{\nu}$ and the precision measurement of $|V_{cb}|$

3.1 Model-independent predictions for the $B \rightarrow D^* \ell \bar{\nu}$ rate at zero recoil

*“The result we proceed to divide, as you see,
By Nine Hundred and Ninety and Two;
Then subtract Seventeen, and the answer must be
Exactly and perfectly true.”*

Lewis Carroll [1]

Hadrons containing one b quark decay mainly into charmed hadrons. Other decay modes (Cabibbo suppressed $b \rightarrow u$ transitions, $B \rightarrow J/\psi X$ decays, etc.) constitute only about 1% of the total decay rate. Among the $b \rightarrow c$ decay modes the exclusive decay $B \rightarrow D^* \ell \bar{\nu}$ is particularly interesting because it offers a possibility to accurately measure the Cabibbo-Kobayashi-Maskawa angle $|V_{cb}|$. The reason is that HQET makes definite predictions for the form factors describing this transition at zero recoil, i.e., when the final state D^* meson has zero velocity in the rest frame of the the initial B meson. In this section we review how the HQET predictions arise. The next section is devoted to the so called zero recoil sum rules. These sum rules, first obtained in Ref. [9] and further investigated in Refs. [25, 26], can be used to estimate the accuracy of the HQET predictions for the form factors.

The form factors for the semileptonic $B \rightarrow D^{(*)} \ell \bar{\nu}$ decay are defined as ¹

$$\begin{aligned}
2 \langle D(v') | V^\mu | B(v) \rangle &= h_+(w)(v + v')^\mu + h_-(w)(v - v')^\mu, \\
2 \langle D^*(v', \epsilon) | V^\mu | B(v) \rangle &= i h_V(w) \epsilon^{\mu\nu\alpha\beta} \epsilon_\nu^* v'_\alpha v_\beta, \\
2 \langle D^*(v', \epsilon) | A^\mu | B(v) \rangle &= h_{A_1}(w)(w + 1) \epsilon^{*\mu} - h_{A_2}(w)(\epsilon^* \cdot v) v^\mu \\
&\quad - h_{A_3}(w)(\epsilon^* \cdot v) v'^\mu.
\end{aligned} \tag{3.1}$$

Here $V^\mu = \bar{c} \gamma^\mu b$ and $A^\mu = \bar{c} \gamma^\mu \gamma_5 b$ are the vector and axial vector currents. (The axial form factor between B and D mesons vanishes identically because of requirements of parity and Lorentz invariance.) The four-velocities of the initial and final states are denoted by v and v' respectively, and $w = v \cdot v'$. The polarization vector of the D^* meson is denoted by ϵ .

The part of the effective weak Lagrangian relevant for semileptonic $b \rightarrow c$ decays reads

$$L_{eff} = G_F \sqrt{2} (V^\mu - A^\mu) \bar{e}_L \gamma_\mu \nu_L, \tag{3.2}$$

where G_F is the Fermi constant. The quark currents V and A have zero anomalous dimension, and therefore the normalization point μ need not be specified.

Given the effective Lagrangian, Eq. (3.2), and the definitions in Eqs. (3.1), one easily finds the differential decay rates:

$$\begin{aligned}
\frac{d\Gamma(B \rightarrow D^* \ell \bar{\nu}_e)}{dw} &= \frac{G_F^2 m_B^5}{48\pi^3} r^{*3} (1 - r^*)^2 (w^2 - 1)^{1/2} (w + 1)^2 \\
&\quad \times \left[1 + \frac{4w}{w + 1} \frac{1 - 2wr^* + r^{*2}}{(1 - r^*)^2} \right] |V_{cb}|^2 |\mathcal{F}_{B \rightarrow D^*}(w)|^2, \\
\frac{d\Gamma(B \rightarrow D \ell \bar{\nu}_e)}{dw} &= \frac{G_F^2 m_B^5}{48\pi^3} r^3 (1 + r)^2 (w^2 - 1)^{3/2} |V_{cb}|^2 |\mathcal{F}_{B \rightarrow D}(w)|^2,
\end{aligned} \tag{3.3}$$

where $r^{(*)} = m_{D^{(*)}}/m_B$. The functions $\mathcal{F}_{B \rightarrow D^*}$ and $\mathcal{F}_{B \rightarrow D}$ are given in terms of the

¹The funny factors of 2 arise because we use the nonrelativistic normalization of states $\langle \mathbf{p}' | \mathbf{p} \rangle = (2\pi)^3 v^0 \delta^3(\mathbf{p} - \mathbf{p}')$.

form factors:

$$\begin{aligned}
|\mathcal{F}_{B \rightarrow D^*}(w)|^2 &= \left[1 + \frac{4w}{w+1} \frac{1 - 2wr^* + r^{*2}}{(1-r^*)^2} \right]^{-1} \\
&\times \left\{ \frac{1 - 2wr^* + r^{*2}}{(1-r^*)^2} 2 \left[h_{A_1}^2(w) + \frac{w-1}{w+1} h_V^2(w) \right] \right. \\
&\quad \left. + \left[h_{A_1}(w) + \frac{w-1}{1-r^*} \left(h_{A_1}(w) - h_{A_3}(w) - r^* h_{A_2}(w) \right) \right]^2 \right\}, \\
\mathcal{F}_{B \rightarrow D}(w) &= h_+(w) - \frac{1-r}{1+r} h_-(w). \tag{3.4}
\end{aligned}$$

We will be interested in the differential rate at vanishingly small recoil, i.e., for $v = v', w = 1$. In this limit

$$|\mathcal{F}_{B \rightarrow D^*}(1)| = |h_{A_1}(1)|, \quad |\mathcal{F}_{B \rightarrow D}(1)| = |h_+(1)|. \tag{3.5}$$

According to Eqs. (2.18,2.21), if one neglects corrections of order $1/m_{c,b}$, the form factors are all expressed through a single function $\xi(w)$ which satisfies $\xi(1) = 1$. In particular, the form factors h_+ and h_{A_1} at zero recoil are given by

$$\begin{aligned}
h_+(1) &= \eta_V \equiv C_V^{(1)}(1, \mu) + C_V^{(2)}(1, \mu) + C_V^{(3)}(1, \mu), \\
h_{A_1}(1) &= \eta_A \equiv C_A^{(1)}(1, \mu), \tag{3.6}
\end{aligned}$$

where the coefficients $C_{A,V}^{(i)}$ are defined in Eq. (2.18).

The quantities η_A and η_V do not depend on the renormalization scale μ . To see why, note that for $v = v'$ we have only one independent operator in HQET which can match onto A_μ , namely $\bar{h}_v^{(c)} \gamma_\mu \gamma_5 h_v^{(b)}$. (For $v \neq v'$ there are three independent operators — see Eq. (2.18).) This operator is actually one of the generators of HQS, and therefore its matrix elements between b and c quark states do not receive any perturbative corrections. Thus the ‘‘HQET side’’ of the matching calculation is trivial in this case. In full theory, the operator A_μ is not conserved, but it is ‘‘partially conserved,’’ i.e., it would be conserved if the quark masses were zero. Partial conservation is enough to ensure that the anomalous dimension of A_μ vanishes in full QCD.

Therefore the matrix elements of A_μ , and consequently the matching coefficient η_A , cannot depend on the subtraction point μ . Similarly, η_V must be μ -independent.

Although the matching coefficients are known only to order α_s , the particular combinations entering Eq. (3.6) have been computed to order α_s^2 [27]. Here we write down an analytic expression for η_A which contains the full order α_s corection and part of the order α_s^2 correction which is proportional to $\beta_0 = 11 - \frac{2}{3}n_f$ (n_f is the number of light quark flavors):

$$\eta_A = 1 - \frac{\alpha_s}{\pi} \left(\frac{m_b + m_c}{m_b - m_c} \ln \frac{m_c}{m_b} + \frac{8}{3} \right) - \frac{\alpha_s^2}{\pi^2} \beta_0 \frac{5}{24} \left(\frac{m_b + m_c}{m_b - m_c} \ln \frac{m_c}{m_b} + \frac{44}{15} \right). \quad (3.7)$$

In Eq. (3.7) α_s is the $\overline{\text{MS}}$ coupling evaluated at the scale $\sqrt{m_b m_c}$. Of course, the complete order α_s^2 contribution [27] contains terms which are not proportional to β_0 . Still, Eq. (3.7) approximates the complete order α_s^2 result very well because β_0 is large numerically. In general, it was noticed that for many QCD observables corrections of order $\alpha_s^2 \beta_0$ provide a good approximation of the full order α_s^2 corrections. Examples can be found in Ref. [28]

Putting all this together, we conclude that up to corrections suppressed by $\Lambda_{\text{QCD}}/m_{c,b}$ the values of $|\mathcal{F}_{B \rightarrow D^*}(1)|$ and $|\mathcal{F}_{B \rightarrow D}(1)|$ are given by η_A and η_V , respectively. Since measuring the differential rates $d\Gamma/dw$ near $w = 1$ is equivalent to measuring $|\mathcal{F}(1)V_{cb}|$ (see Eq. (3.3)), we can extract the value of $|V_{cb}|$ by studying the decays $B \rightarrow D\ell\bar{\nu}$ or $B \rightarrow D^*\ell\bar{\nu}$.

In real life m_c is not very large, and the corrections of order $1/m_c$ may be quite substantial. However, Luke's theorem [29] states that for $B \rightarrow D^*$ decay there are *no* corrections of order $1/m_{c,b}$. There are still corrections of order $1/m_{c,b}^2$, and they limit the accuracy of the extraction. The corresponding theoretical uncertainty is expected to be of order $(\Lambda/2m_c)^2$, where Λ is the characteristic scale of strong interactions. Setting $\Lambda = 0.5$ GeV, $m_c = 1.4$ GeV, we conclude that $1/m_c^2$ corrections to the value of $|\mathcal{F}_{B \rightarrow D^*}(1)|$ are of order 3%. Therefore the theoretical uncertainty of the extraction of $|V_{cb}|$ is also of order 3%. (Of course, "of order 3%" may mean 6% or even 10% in practice.)

Naturally, one would like to know better the size of $1/m_{c,b}^2$ corrections. Unfortunately, this cannot be done in a model-independent manner. In Ref. [30] the $1/m_c^2$ contribution enhanced by the logarithm $\log \Lambda_{\text{QCD}}/m_\pi$ has been evaluated using chiral perturbation theory. It turned out to be negative and small, less than 0.7% in absolute value. Although formally this logarithmically enhanced contribution “dominates,” its tiny value suggests that the nonlogarithmic contributions cannot be neglected. Another approach is based on zero recoil sum rules [9]. These sum rules can be used to put an upper bound on $|\mathcal{F}_{B \rightarrow D^*}(1)|$. Under favourable circumstances, this bound may provide information on the deviation of $|\mathcal{F}_{B \rightarrow D^*}(1)|$ from η_A . In addition, the zero recoil sum rules constrain the matrix element λ_1 . In the next section we review both applications following mostly Ref. [26].

3.2 Zero recoil sum rules

But the Judge said he never had summed up before;

So the Snark undertook it instead,

And summed it so well that it came to far more

Than the Witnesses ever had said.

Lewis Carroll [1]

The zero recoil sum rules follow from analysis of the time ordered product ²

$$T_{\mu\nu} = i \int d^4x e^{-iq \cdot x} \langle B | T \{ J_\mu^\dagger(x), J_\nu(0) \} | B \rangle, \quad (3.8)$$

where $J_\nu = A_\nu$ or V_ν , and the B states are at rest, $\vec{q} = 0$ and $q^0 = m_b - m_c - \epsilon$. Viewed as a function of complex ϵ , $T_{\mu\nu}$ has two cuts along the real ϵ -axis. One, for $\epsilon > 0$, corresponds to physical states with a charm quark and the other, for $\epsilon < -2m_c$, corresponds to physical intermediate states with two b quarks and a \bar{c} quark. The

²Gentle Reader! The following discussion is very lengthy and technical. You may want to skip it and jump to page 37, where the disappointing conclusions are stated.

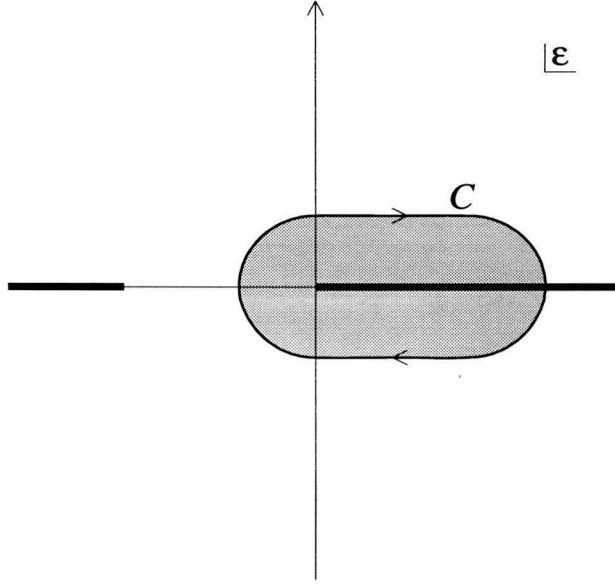


Figure 3.1: The integration contour C in the complex ϵ plane. The cuts extend to $\text{Re } \epsilon \rightarrow \pm\infty$.

first cut arises from inserting the states between the two currents in the product $J^\dagger J$, and the second cut arises from inserting the states between the currents in the other time ordering $J J^\dagger$. So we arrive at

$$\begin{aligned}
 T_{\mu\nu}(\epsilon) &= \sum_X (2\pi)^3 \delta^3(\vec{p}_X) \frac{\langle B|J_\mu^\dagger|X\rangle\langle X|J_\nu|B\rangle}{(m_b - m_c) - (m_B - m_X) - \epsilon - i0} \\
 &- \sum_X (2\pi)^3 \delta^3(\vec{p}_X) \frac{\langle B|J_\nu|X\rangle\langle X|J_\mu^\dagger|B\rangle}{(m_b - m_c) + (m_B - m_X) - \epsilon + i0}. \quad (3.9)
 \end{aligned}$$

The sum over X includes the usual phase space factors, i.e., $d^3p/(2\pi)^3$ for each particle in the state X .

Consider the integral of the product of a weight function $W_\Delta(\epsilon)$ with $T_{\mu\nu}(\epsilon)$ along the contour C shown in Fig. 3.1. Assuming W is analytic in the shaded region enclosed by this contour and averaging over $\mu = \nu = 1, 2, 3$, we get

$$\frac{1}{2\pi i} \int_C d\epsilon W_\Delta(\epsilon) \frac{T_{ii}(\epsilon)}{3} = \sum_X W_\Delta[(m_X - m_c) - (m_B - m_b)] (2\pi)^3 \delta^3(\vec{p}_X) \frac{|\langle X|J_i|B\rangle|^2}{3}. \quad (3.10)$$

The maximum X mass on the right-hand side of Eq. (3.10) is determined by where the contour C pinches the real axis. For convenience this mass is chosen to be less than $2m_b + m_c$ to prevent the occurrence of states X with b , \bar{b} , and c quarks. We take the maximum X mass to be $2m_B$ and then Eq. (3.10) relies on local duality [21] at this scale. Hereafter it is understood that sums over X only go over states up to mass $2m_B$.

We require that: (i) the weight function W_Δ be positive semidefinite along the cut so that every term in the sum over X on the right-hand side of Eq. (3.10) is non-negative; (ii) $W_\Delta(0) = 1$; (iii) W_Δ be flat near $\epsilon = 0$, i.e., $dW_\Delta(\epsilon)/d\epsilon|_{\epsilon=0} = 0$; (iv) and that it falls off rapidly to zero for $\epsilon > \Delta$. We want to take $\Delta \ll m_{c,b}$. Then states X other than the D^* give a contribution to the right-hand side of Eq. (3.10) that is suppressed by $(1/m_{c,b})^2$. However, in our numerical results we consider Δ as large as 2 GeV. Although our analysis holds for any weight function that satisfies these four properties, for explicit calculations we use

$$W_\Delta^{(n)}(\epsilon) = \frac{\Delta^{2n}}{\epsilon^{2n} + \Delta^{2n}}, \quad (3.11)$$

with $n = 2, 3, \dots$ (for $n = 1$ the integral over ϵ is dominated by contributions from states with mass of order m_B). These weight functions have poles at $\epsilon = \sqrt[2n]{-1} \Delta$, therefore, as long as n is not too large and Δ is much larger than the QCD scale, Λ_{QCD} , the contour in Fig. 3.1 is far from the cut until ϵ is near $2m_B$. Then we should be able to calculate the integral in Eq. (3.10) using the operator product expansion to evaluate the time ordered product.

The choice of the set of weight functions in Eq. (3.11) is motivated by the fact that for values of n of order unity all poles of $W_\Delta^{(n)}$ lie at a distance of order Δ away from the physical cut. In this case the integral along the contour C can be computed assuming local duality at the scale $2m_B$. The dependence of our results on this assumption is extremely weak, because for $\Delta \ll m_B$ the weight function is very small where the contour C touches the cut. As $n \rightarrow \infty$, $W_\Delta^{(n)}$ approaches $\theta(\Delta - \epsilon)$ for positive ϵ , which corresponds to summing over all hadronic resonances

up to excitation energy Δ with equal weight. Then the poles of $W_\Delta^{(n)}$ approach the cut, and the contour C is forced to lie within a distance of order Δ/n from the cut at $\epsilon = \Delta$. In this case the evaluation of the integral along the contour C relies also on local duality at the scale Δ .³

Neglecting perturbative QCD corrections and nonperturbative effects corresponding to operators of dimension greater than five, the operator product expansion gives [31]

$$\frac{1}{3} T_{ii}^{AA} = -\frac{1}{\epsilon} + \frac{(\lambda_1 + 3\lambda_2)(m_b - 3m_c)}{6m_b^2 \epsilon (2m_c + \epsilon)} - \frac{4\lambda_2 m_b - (\lambda_1 + 3\lambda_2)(m_b - m_c - \epsilon)}{m_b \epsilon^2 (2m_c + \epsilon)}, \quad (3.12)$$

when $J_\mu = A_\mu = \bar{c} \gamma_\mu \gamma_5 b$, and

$$\frac{1}{3} T_{ii}^{VV} = -\frac{1}{2m_c + \epsilon} + \frac{(\lambda_1 + 3\lambda_2)(m_b + 3m_c)}{6m_b^2 \epsilon (2m_c + \epsilon)} - \frac{4\lambda_2 m_b - (\lambda_1 + 3\lambda_2)(m_b - m_c - \epsilon)}{m_b \epsilon (2m_c + \epsilon)^2}, \quad (3.13)$$

when $J_\mu = V_\mu = \bar{c} \gamma_\mu b$. Performing the contour integration yields

$$\begin{aligned} \frac{1}{3} \sum_X W_\Delta [(m_X - m_c) - (m_B - m_b)] (2\pi)^3 \delta^3(\vec{p}_X) |\langle X | A_i | B \rangle|^2 \\ = 1 - \frac{\lambda_2}{m_c^2} + \left(\frac{\lambda_1 + 3\lambda_2}{4} \right) \left(\frac{1}{m_c^2} + \frac{1}{m_b^2} + \frac{2}{3m_c m_b} \right), \end{aligned} \quad (3.14)$$

$$\begin{aligned} \frac{1}{3} \sum_X W_\Delta [(m_X - m_c) - (m_B - m_b)] (2\pi)^3 \delta^3(\vec{p}_X) |\langle X | V_i | B \rangle|^2 \\ = \frac{\lambda_2}{m_c^2} - \left(\frac{\lambda_1 + 3\lambda_2}{4} \right) \left(\frac{1}{m_c^2} + \frac{1}{m_b^2} - \frac{2}{3m_c m_b} \right). \end{aligned} \quad (3.15)$$

These equations hold for any W_Δ that satisfies the four properties mentioned above. Higher order terms in the operator product expansion for T_{ii} give contributions with more factors of $1/\epsilon$ on the right-hand sides of Eqs. (3.12) and (3.13). Therefore, if the weight function has nonvanishing m 'th derivative at $\epsilon = 0$, there are corrections

³In fact, for any sequence of functions analytic in some neighbourhood of the positive real axis that converges to $\theta(\Delta - \epsilon)$, some singularity will approach $\epsilon = \Delta$. Thus, the pinching of the contour is inevitable if one uses a weight function that varies rapidly.

to the right-hand side of Eq. (3.14) of order

$$\left(\frac{\Lambda_{\text{QCD}}}{m_{c,b}}\right)\left(\frac{\Lambda_{\text{QCD}}}{\Delta}\right)^m = \left(\frac{\Lambda_{\text{QCD}}}{m_{c,b}}\right)^2 \left[\left(\frac{m_{c,b}}{\Lambda_{\text{QCD}}}\right)\left(\frac{\Lambda_{\text{QCD}}}{\Delta}\right)^m\right]. \quad (3.16)$$

We require that Δ be large enough compared with Λ_{QCD} so that such terms are smaller than those we kept in Eq. (3.14). For $m > 1$, Δ can still be smaller than $m_{c,b}$. Higher order terms in the operator product expansion of T_{ii}^{VV} give corrections to the right-hand side of Eq. (3.15) of order $(\Lambda_{\text{QCD}}/m_{c,b})^2 (\Lambda_{\text{QCD}}/\Delta)^{m-1}$. This is why we imposed condition (iii). For the weight function $W_{\Delta}^{(n)}(\epsilon)$ in Eq. (3.11) the first nonvanishing derivative is at $m = 2n$.

We have considered the nonperturbative contributions to the sum rules characterized by λ_1 and λ_2 . There are also perturbative corrections suppressed by powers of the strong coupling. These are most easily calculated not in the operator product expansion, but by directly considering the sum over states in Eqs. (3.14, 3.15) and replacing the hadronic states by quark and gluon states. The perturbative corrections are of two types. There are corrections of order $\alpha_s(m_{c,b})$ not suppressed by powers of $\Delta/m_{c,b}$. These arise, at the parton level, from the final state $X = c$ and change the term 1 on the right-hand side of Eq. (3.14) to η_A^2 .

There is another class of perturbative QCD corrections coming from final states X that contain a charm quark plus additional partons, e.g., cg , $c\bar{q}q$, etc. They give a contribution to the right-hand side of Eqs. (3.14, 3.15) which is of order $[\alpha_s(\Delta) + \dots] F(\Delta)$, where the ellipses denote terms of higher order in the strong coupling constant α_s , and for small Δ , $F(\Delta) \sim \Delta^2/m_{c,b}^2$. We have evaluated the strong coupling constant at the scale Δ , because this scale characterizes the typical hadronic mass in the sum over X . Note that, although these corrections are suppressed by powers of $\Delta/m_{c,b}$, they can be as important as the other perturbative corrections we considered since the strong coupling constant is evaluated at a lower scale Δ . The value for these corrections depends on the precise form of the weight function. We use the ones given in Eq. (3.11). Such perturbative corrections were calculated in Refs. [9, 32] at order $\alpha_s(\Delta) \Delta^2/m_{c,b}^2$ in the limit when the weight function approaches

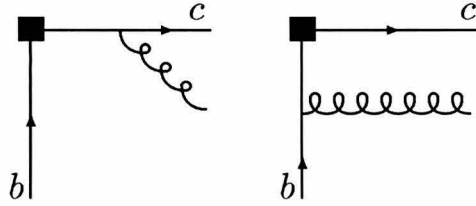


Figure 3.2: Feynman diagrams that contribute to the order $\alpha_s(\Delta)$ corrections to the sum rules. The black square indicates insertion of the $b \rightarrow c$ axial or vector current.

the step-function $\theta(\Delta - \epsilon)$ (corresponding to $W_\Delta^{(\infty)}$). As already pointed out, the use of such a weight function relies on local duality at the scale Δ , so the corrections are expected to be less than those stemming from $W_\Delta^{(n)}$ with small n relying on local duality only at the scale $2m_B$. For $n \geq 2$ the order $\alpha_s(\Delta)$ terms coming from the Feynman diagrams in Fig. 3.2, and the order $\alpha_s^2(\Delta) \beta_0$ terms arising from the diagrams in Fig. 3.3 were computed in Ref. [26]. The rationale for computing only the part of the α_s^2 contribution proportional to β_0 is that in most known examples it is the dominant part of the full α_s^2 contribution. Taking into account these perturbative corrections, Eqs. (3.14,3.15) become

$$\begin{aligned}
& \frac{1}{3} \sum_X W_\Delta^{(n)} [(m_X - m_c) - (m_B - m_b)] (2\pi)^3 \delta^3(\vec{p}_X) \left| \langle X | A_i | B \rangle \right|^2 \\
&= \eta_A^2 - \frac{\lambda_2}{m_c^2} + \left(\frac{\lambda_1 + 3\lambda_2}{4} \right) \left(\frac{1}{m_c^2} + \frac{1}{m_b^2} + \frac{2}{3m_c m_b} \right) \\
&+ \frac{\alpha_s(\Delta)}{\pi} X_{AA}^{(n)}(\Delta) + \frac{\alpha_s^2(\Delta)}{\pi^2} \beta_0 Y_{AA}^{(n)}(\Delta), \tag{3.17}
\end{aligned}$$

$$\begin{aligned}
& \frac{1}{3} \sum_X W_\Delta^{(n)} [(m_X - m_c) - (m_B - m_b)] (2\pi)^3 \delta^3(\vec{p}_X) \left| \langle X | V_i | B \rangle \right|^2 \\
&= \frac{\lambda_2}{m_c^2} - \left(\frac{\lambda_1 + 3\lambda_2}{4} \right) \left(\frac{1}{m_c^2} + \frac{1}{m_b^2} - \frac{2}{3m_c m_b} \right) \\
&+ \frac{\alpha_s(\Delta)}{\pi} X_{VV}^{(n)}(\Delta) + \frac{\alpha_s^2(\Delta)}{\pi^2} \beta_0 Y_{VV}^{(n)}(\Delta). \tag{3.18}
\end{aligned}$$

On the right-hand sides of Eqs. (3.17,3.18) terms suppressed by more than two

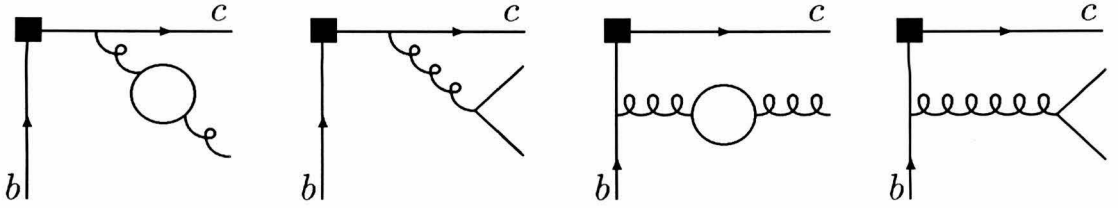


Figure 3.3: Feynman diagrams that determine the order $\alpha_s^2(\Delta)\beta_0$ corrections to the sum rules.

powers of $\Lambda_{\text{QCD}}/m_{c,b}$ or α_s have been neglected. We have also neglected in Eq. (3.17) terms suppressed by $(\Lambda_{\text{QCD}}/m_{c,b})(\Lambda_{\text{QCD}}/\Delta)^{2n}$ and in Eq. (3.18) terms suppressed by $(\Lambda_{\text{QCD}}/m_{c,b})^2(\Lambda_{\text{QCD}}/\Delta)^{2n-1}$. Perturbative corrections to the terms proportional to $\lambda_{1,2}$ are also neglected, and we evaluate λ_2 in Eqs. (3.17,3.18) at the scale Δ so that QCD corrections to its coefficient do not contain any large logarithms. For $\Delta \ll m_{c,b}$ the functions $X^{(n)}$ and $Y^{(n)}$ are given by

$$\begin{aligned}
X_{AA}^{(n)}(\Delta) &= \Delta^2 \frac{A^{(n)}}{3} \left(\frac{1}{m_c^2} + \frac{1}{m_b^2} + \frac{2}{3m_c m_b} \right), \\
X_{VV}^{(n)}(\Delta) &= \Delta^2 \frac{A^{(n)}}{3} \left(\frac{1}{m_c^2} + \frac{1}{m_b^2} - \frac{2}{3m_c m_b} \right), \\
Y_{AA}^{(n)}(\Delta) &= \Delta^2 \frac{B^{(n)}}{6} \left(\frac{1}{m_c^2} + \frac{1}{m_b^2} + \frac{2}{3m_c m_b} \right) + \Delta^2 \frac{A^{(n)}}{15} \left(\frac{1}{m_c^2} + \frac{1}{m_b^2} + \frac{4}{3m_c m_b} \right), \\
Y_{VV}^{(n)}(\Delta) &= \Delta^2 \frac{B^{(n)}}{6} \left(\frac{1}{m_c^2} + \frac{1}{m_b^2} - \frac{2}{3m_c m_b} \right), \tag{3.19}
\end{aligned}$$

where the coefficients $A^{(n)}$ and $B^{(n)}$ are ($n \geq 2$)

$$A^{(n)} = \frac{\pi}{n \sin(\pi/n)}, \quad B^{(n)} = A^{(n)} \left(\frac{\pi}{2n \tan(\pi/n)} + \frac{5}{3} - \ln 2 \right). \tag{3.20}$$

For Δ near 1 GeV higher powers of $\Delta/m_{c,b}$ are important. The analytic expressions for $X_{AA}^{(\infty)}$ and $X_{VV}^{(\infty)}$ are (for $\Delta < 2m_b$)

$$\begin{aligned}
X_{AA}^{(\infty)} &= \frac{\Delta(\Delta + 2m_c)[2(\Delta + m_c)^2 - 2m_b^2 - (m_b + m_c)^2]}{18m_b^2(\Delta + m_c)^2} \\
&\quad + \frac{3m_b^2 + 2m_b m_c - m_c^2}{9m_b^2} \ln \frac{\Delta + m_c}{m_c},
\end{aligned}$$

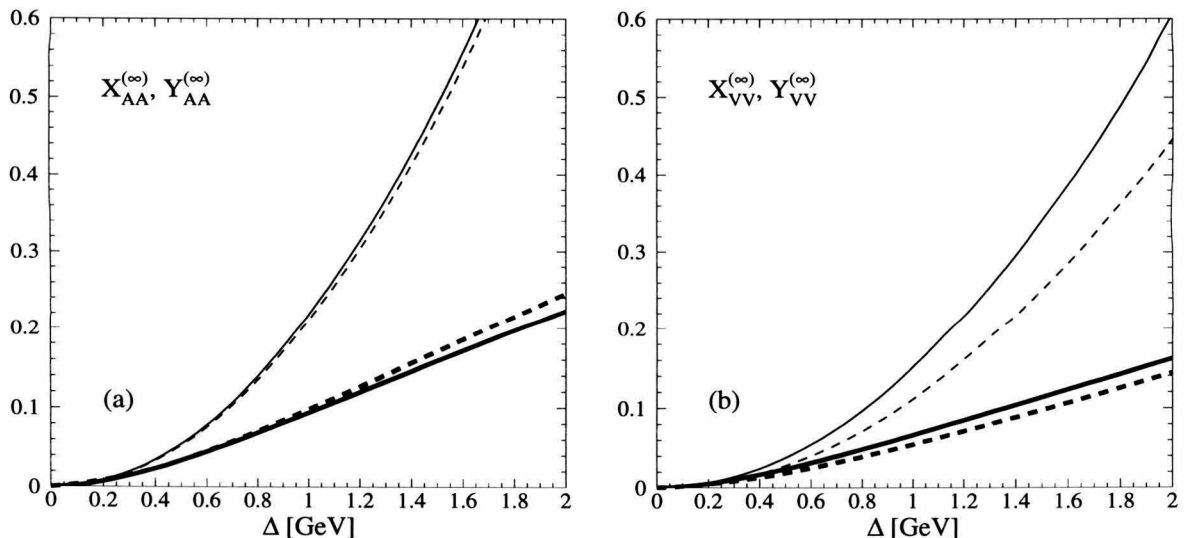


Figure 3.4: $X^{(\infty)}(\Delta)$ and $Y^{(\infty)}(\Delta)$ for the a) axial, and b) vector coefficients. Thick solid lines are X while thick dashed lines are Y . The thin solid and dashed lines are X and Y to order $\Delta^2/m_{c,b}^2$.

$$\begin{aligned}
 X_{VV}^{(\infty)} = & \frac{\Delta (\Delta + 2m_c) [2(\Delta + m_c)^2 - 2m_b^2 - (m_b - m_c)^2]}{18m_b^2 (\Delta + m_c)^2} \\
 & + \frac{3m_b^2 - 2m_b m_c - m_c^2}{9m_b^2} \ln \frac{\Delta + m_c}{m_c}. \quad (3.21)
 \end{aligned}$$

In Fig. 3.4 we plot $X^{(\infty)}$ and $Y^{(\infty)}$ versus Δ using the values $m_b = 4.8$ GeV and $m_c = 1.4$ GeV. The thick solid lines are X and the thick dashed lines are Y , while the thin lines are the corresponding functions at order $\Delta^2/m_{c,b}^2$. Note that expanding in $\Delta/m_{c,b}$ is not a good approximation unless $\Delta < 400$ MeV.

The evaluation of the order $\alpha_s^2 \beta_0$ corrections is made relatively simple by the relation between the n_f dependent part of the order α_s^2 contribution and the order α_s contribution with a finite gluon mass [33]. Such a relation holds in the so-called V -scheme, but throughout this paper we present all results in the usual $\overline{\text{MS}}$ scheme. Knowledge of the order $\alpha_s^2 \beta_0$ corrections allows us to obtain the BLM scale [34] that results from absorbing vacuum polarization effects into the running coupling constant. It is generally believed that this choice of scale yields a reasonable perturbative expansion. This is also the reason for using $\alpha_s(\Delta)$ in the sum rules in Eqs. (3.17, 3.18).

Had we chosen some very different scale μ , the coefficients $Y^{(n)}$ would contain large logarithms of μ^2/Δ^2 . On the other hand, the “natural” scale for the perturbative corrections to the sum rules coming from η_A^2 is $\sqrt{m_c m_b}$.

The sum rule in Eq. (3.17) implies a bound on the zero recoil $B \rightarrow D^*$ matrix element of the axial current $\mathcal{F}_{B \rightarrow D^*}(1)^2$, defined by $\langle D^* | A_i | B \rangle = \mathcal{F}_{B \rightarrow D^*}(1) \varepsilon_i$:

$$|\mathcal{F}_{B \rightarrow D^*}(1)|^2 \leq \eta_A^2 - \frac{\lambda_2}{m_c^2} + \left(\frac{\lambda_1 + 3\lambda_2}{4} \right) \left(\frac{1}{m_c^2} + \frac{1}{m_b^2} + \frac{2}{3m_c m_b} \right) + \frac{\alpha_s(\Delta)}{\pi} X_{AA}^{(n)}(\Delta) + \frac{\alpha_s^2(\Delta)}{\pi^2} \beta_0 Y_{AA}^{(n)}(\Delta). \quad (3.22)$$

Here we used the fact that the contributions of states X of higher mass than the D^* to the left-hand side of Eq. (3.17) are positive, and neglected the very small deviation of $W_\Delta^{(n)}[(m_{D^*} - m_c) - (m_B - m_b)]$ from unity implied by Eq. (3.11), Eq. (2.14), and the relation $m_{D^*} - m_D = 2\lambda_2/m_c$. The positivity of the sum over states X in Eq. (3.18) implies that

$$0 \leq \frac{\lambda_2}{m_c^2} - \left(\frac{\lambda_1 + 3\lambda_2}{4} \right) \left(\frac{1}{m_c^2} + \frac{1}{m_b^2} - \frac{2}{3m_c m_b} \right) + \frac{\alpha_s(\Delta)}{\pi} X_{VV}^{(n)}(\Delta) + \frac{\alpha_s^2(\Delta)}{\pi^2} \beta_0 Y_{VV}^{(n)}(\Delta). \quad (3.23)$$

This inequality gives a constraint on the heavy quark effective theory matrix element λ_1 , which is strongest if one takes the $m_c \gg m_b \gg \Delta$ limit, giving

$$\lambda_1 \leq -3\lambda_2 + \frac{\alpha_s(\Delta)}{\pi} \Delta^2 \frac{4A^{(n)}}{3} + \frac{\alpha_s^2(\Delta)}{\pi^2} \beta_0 \Delta^2 \frac{2B^{(n)}}{3}. \quad (3.24)$$

(Since the HQET matrix elements are independent of m_c and m_b , and the inequality in Eq. (3.23) is valid even for unphysical values of m_c and m_b , one is free to take the limit $m_c \gg m_b \gg \Delta$.)

Let us now use these bounds to investigate the size of the $1/m_c^2$ corrections to the form factor at zero recoil $|\mathcal{F}_{B \rightarrow D^*}(1)|$. First we would like to know how to choose Δ . The bound in Eq. (3.22) is more restrictive for small Δ , when only a few states other than D^* can contribute to the right-hand side of Eq. (3.17). But for Δ of order Λ_{QCD} or lower perturbation theory in $\alpha_s(\Delta)$ cannot be trusted. Thus we must

determine the smallest value of Δ for which perturbative corrections to the sum rule Eq. (3.17) are still under control. To do this consistently, we must reexpand η_A from Eq. (3.7) in powers of $\alpha_s(\Delta)$. The result is that for Δ as low as 1 GeV the perturbative corrections to the sum rule seem to be under control. For example, for $\Delta = 1$ GeV, $m_c = 1.4$ GeV, $m_b = 4.8$ GeV, and $\alpha_s(1 \text{ GeV}) = 0.52$ we obtain the following series:

$$1 - \frac{\alpha_s(1\text{GeV})}{\pi} 0.75 + \frac{\alpha_s(1\text{GeV})^2 \beta_0}{\pi^2} 0.20 + \dots = 1 - 0.12 + 0.05 + \dots \quad (3.25)$$

This series appears to be convergent. Alternatively, one can compute the BLM scale by absorbing the order $\alpha_s^2 \beta_0$ correction in Eq. (3.25) into the order α_s correction. The BLM scale turns out to be 1.7 GeV, which appears to be high enough for perturbation theory to work. Thus we use $\Delta = 1$ GeV in the bound Eq. (3.22) in what follows.

Eq. (3.25) suggests that for $\Delta = 1$ GeV the uncertainty on the right-hand side of Eq. (3.22) due to neglecting higher order perturbative corrections is less than 5%. Then it makes sense to include nonperturbative corrections as well. It so happens that the coefficient of λ_2 in Eq. (3.22) is very small for physical values of m_c and m_b , and therefore the corresponding contribution is negligible. Not so for λ_1 ! The bound in Eq. (3.22) now reads

$$|\mathcal{F}_{B \rightarrow D^*}(1)|^2 < 0.93 + \frac{\lambda_1}{6.1 \text{ GeV}^2}. \quad (3.26)$$

Unfortunately the value of λ_1 is poorly known at present. Estimates based on QCD sum rules range from -0.1 GeV^2 to -0.6 GeV^2 . In the next chapter we will see that experimental data on inclusive semileptonic B decays give values for λ_1 anywhere from 0.1 GeV^2 to -0.6 GeV^2 . It seems that at present the only relatively safe bet is that λ_1 is negative. Then the bound becomes $|\mathcal{F}_{B \rightarrow D^*}(1)| < 0.965$. On the other hand, $\eta_A \simeq 0.95$ (we take $m_c = 1.4$ GeV, $m_b = 4.8$ GeV, $\alpha_s(M_Z) = 0.117$). Thus the bound does not provide any information on the deviation of $|\mathcal{F}_{B \rightarrow D^*}(1)|$ from η_A .

Let us now turn to the bound in Eq. (3.24) for the matrix element λ_1 . If one omits perturbative corrections in Eq. (3.24), the bound becomes $\lambda_1 < -3\lambda_2$. Since

$\lambda_2 \simeq 0.12 \text{ GeV}^2$, this would mean that λ_1 is negative and larger than 0.36 GeV^2 in absolute value. But once perturbative corrections to the sum rule are included, it turns out to be impossible to obtain any useful information on λ_1 from Eq. (3.24). Indeed, one can easily see that the perturbative corrections on the right-hand side of Eq. (3.24) are under control only for $\Delta > 4 \text{ GeV}$, since the BLM scale is only 0.17Δ . For $\Delta = 4 \text{ GeV}$ Eq. (3.24) only implies

$$\lambda_1 < 1 \text{ GeV}^2. \quad (3.27)$$

This is not a very interesting constraint, since we know anyway that large and positive values of λ_1 are ruled out by the experimental data on the lepton spectrum in the inclusive B decays [35, 11].

We discussed only the bounds following from the sum rules Eqs. (3.17,3.18) with $n = \infty$. It is easy to see that the corresponding bounds for finite n are even less informative than for $n = \infty$, since the weight function $W^{(n)}(\epsilon)$ suppresses the contribution of the highly excited states on the right-hand sides of Eqs. (3.17,3.18) less efficiently than $W^{(\infty)}(\epsilon)$. Numerically, the difference between $n = \infty$ and $1 < n < \infty$ bounds turns out to be rather small.

In the future, if λ_1 turns out to be negative and large, the bound in Eq. (3.26) may become informative. Alternatively, one can try to estimate the contributions of the excited states on the right-hand side of Eq. (3.17) using some model. The contribution of the resonances (radially excited D mesons) can be estimated in the nonrelativistic quark models, e.g., in the ISGW model [36]. It is not clear how to treat the contributions of the multiparticle states, and therefore we will not attempt to do it here.

The conclusion is that zero recoil sum rules, beautiful as they are, do not provide any model independent information on the size of the $1/m_c^2$ corrections to the prediction $|\mathcal{F}_{B \rightarrow D^*}(1)| \simeq \eta_A$, contrary to what is claimed in Ref. [9]. On general grounds we expect the $1/m_c^2$ corrections to be of order 3%, or maybe 6%, as explained in the paragraphs following Eq. (3.7).

Now we are ready to make contact with experiment and deduce the value of $|V_{cb}|$. Taking $m_b = 4.8 \pm 0.2 \text{ GeV}$, $m_b - m_c = 3.39 \pm 0.08 \text{ GeV}$, $\alpha_s(M_Z) = 0.117 \pm 0.004$, we get $\eta_A = 0.953 \pm 0.013$. The quoted error includes the uncertainties in m_c, m_b, α_s , as well as the error due to higher order perturbative corrections (it is conservatively estimated as size of the α_s^2 contribution to η_A [27]). Taking the error due to $1/m_c^2$ corrections to Luke's theorem to be 6%, we obtain

$$|\mathcal{F}_{B \rightarrow D^*}(1)| = 0.953 \pm 0.070. \quad (3.28)$$

The most accurate experimental results on the $B \rightarrow D^* \ell \bar{\nu}$ decay come from ALEPH and CLEO:

$$|\mathcal{F}_{B \rightarrow D^*}(1)V_{cb}| = \begin{cases} (31.9 \pm 1.8(\text{stat}) \pm 1.9(\text{syst})) \times 10^{-3} & [37] \\ (35.1 \pm 1.9(\text{stat}) \pm 1.8(\text{syst}) \pm 0.8(\text{lifetime})) \times 10^{-3} & [38] \end{cases} \quad (3.29)$$

The weighted average of these two measurements is $|\mathcal{F}_{B \rightarrow D^*}(1)V_{cb}| = (33.4 \pm 1.9) \times 10^{-3}$. Combining it with our estimate of $|\mathcal{F}_{B \rightarrow D^*}(1)|$ yields

$$|V_{cb}| = (35.0 \pm 2.0(\text{exp}) \pm 2.6(\text{theor})) \times 10^{-3}. \quad (3.30)$$

From our discussion it should be clear that it is very hard to further reduce the theoretical uncertainty of this measurement of V_{cb} . In the next chapter we will see that studying *inclusive* semileptonic decays of B mesons offers a way to extract V_{cb} which may have smaller theoretical uncertainties.

Chapter 4 The uses of the inclusive

$B \rightarrow X_c \ell \bar{\nu}$ decays

4.1 The theory of the inclusive $B \rightarrow X_c \ell \bar{\nu}$ decays

“The thing can be done,” said the Butcher, “I think.

The thing must be done, I am sure.

The thing shall be done! Bring me paper and ink,

The best there is time to procure.”

Lewis Carroll [1]

In this section we describe the theory of the inclusive semileptonic $B \rightarrow X_c \ell \bar{\nu}$ decays, with ℓ being e or μ . Using the Heavy Quark Expansion discussed in Section 2.2 we derive formulae for the charged lepton spectrum, and the hadron energy and invariant mass spectrum. The results have the form of a double expansion in powers of Λ_{QCD}/m_b and α_s . The leading terms and the order α_s perturbative corrections to it can be computed in the parton model [39, 40]. The first nonperturbative correction is of order $(\Lambda_{\text{QCD}}/m_b)^2$ and can be expressed in terms of the HQET matrix elements λ_1 and λ_2 [20, 41, 42].¹ We also compute the order $(\Lambda_{\text{QCD}}/m_b)^3$ nonperturbative corrections following Ref. [11]. They are parametrized by the matrix elements of two local and four nonlocal dimension-six operators. We do not consider the “mixed” corrections, suppressed both by α_s and $(\Lambda_{\text{QCD}}/m_b)^n$, $n \geq 2$. In the next section we compare these results with the available experimental data. The charged lepton spectrum in the $B \rightarrow X_c e \bar{\nu}$ and $B \rightarrow X_c \mu \bar{\nu}$ decays has been measured accurately by

¹This is true if the leading term is written in terms of the quark masses m_b and m_c . If one rewrites it in terms of the hadron masses m_B and m_D using Eq. (2.14), there *will be* corrections of order Λ_{QCD}/m_B proportional to $\bar{\Lambda}$.

CLEO [43, 44]. Since the theoretical prediction for the shape of the spectrum depends on the quark masses and the HQET parameters λ_1 and λ_2 , one can try to extract their values using the CLEO data. The result is an allowed region in the plane of the HQET parameters $\bar{\Lambda}$ and λ_1 (we regard λ_2 as known from the measured $B - B^*$ mass splitting). Since $\bar{\Lambda}$, λ_1 , and λ_2 parametrize the difference between the quark masses and the hadron masses (see Eq. (2.14)), this amounts to determining m_b and m_c . Finally, we use our values for m_b and m_c to extract $|V_{cb}|$ from the measured total $B \rightarrow X_c \ell \bar{\nu}$ rate.

The effective Hamiltonian density responsible for $b \rightarrow c \ell \bar{\nu}$ decays is

$$H_W = -V_{cb} \frac{4G_F}{\sqrt{2}} J^\mu J_{\ell\mu}, \quad (4.1)$$

where $J^\mu = \bar{c}_L \gamma^\mu b_L$ is the left-handed quark current, and $J_\ell^\mu = \bar{\ell}_L \gamma^\mu \nu_L$ is the left-handed lepton current. The differential decay rate is determined by the hadronic tensor

$$W^{\mu\nu} = (2\pi)^3 \sum_{X_c} \delta^4(p_B - q - p_{X_c}) \langle B(v) | J^{\nu\dagger} | X_c \rangle \langle X_c | J^\mu | B(v) \rangle, \quad (4.2)$$

which can be expanded in terms of five form factors:

$$W^{\mu\nu} = -g^{\mu\nu} W_1 + v^\mu v^\nu W_2 - i\epsilon^{\mu\nu\alpha\beta} v_\alpha q_\beta W_3 + q^\mu q^\nu W_4 + (q^\mu v^\nu + q^\nu v^\mu) W_5. \quad (4.3)$$

Then the differential semileptonic decay rate is given by

$$\frac{d\Gamma}{dq^2 dE_\ell dE_\nu} = \frac{96 \Gamma_0}{m_b^5} \left(W_1 q^2 + W_2 \left(2E_\ell E_\nu - \frac{1}{2} q^2 \right) + W_3 q^2 (E_\ell - E_\nu) \right) \times \theta(E_\ell) \theta(E_\nu) \theta(q^2) \theta(4E_\ell E_\nu - q^2). \quad (4.4)$$

Here Γ_0 is the spectator model total decay rate in the limit of zero charm mass

$$\Gamma_0 = |V_{cb}|^2 G_F^2 \frac{m_b^5}{192\pi^3}. \quad (4.5)$$

We have neglected the lepton mass, which is a very good approximation for $\ell = e$ or

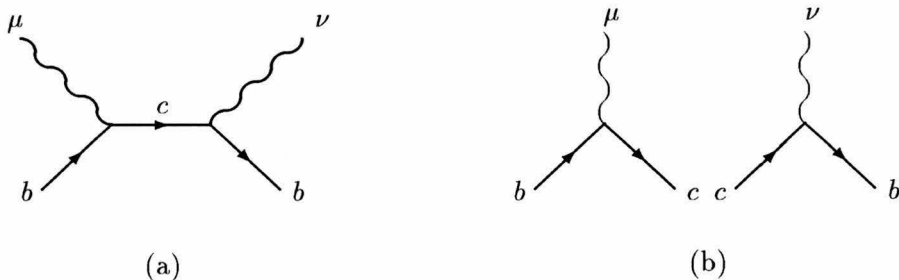


Figure 4.1: (a) The relevant term in the operator product expansion. Wavy lines denote the insertions of left-handed currents. (b) does not contribute to $b \rightarrow c$ decay.

μ .

Defining the current correlator $T^{\mu\nu}$ by

$$\begin{aligned} T^{\mu\nu} &= -i \int d^4x e^{-iq \cdot x} \langle B(v) | T [J^{\nu\dagger}(x) J^\mu(0)] | B(v) \rangle \\ &= -g^{\mu\nu} T_1 + v^\mu v^\nu T_2 - i \epsilon^{\mu\nu\alpha\beta} v_\alpha q_\beta T_3 + q^\mu q^\nu T_4 + (q^\mu v^\nu + q^\nu v^\mu) T_5, \end{aligned} \quad (4.6)$$

one can easily see that $W_i = -\frac{1}{\pi} \text{Im} T_i$. Away from the physical cut $T^{\mu\nu}$ can be computed using the OPE. Then the arguments of Section 2.2 show that the smeared differential decay rate is correctly reproduced by the OPE calculation, provided the width of the smearing function is large enough.

At tree level the only diagram which has a discontinuity across the physical cut is the one in Fig. 4.1a. The corresponding contribution to the time-ordered product is

$$\begin{aligned} &\bar{b} \gamma^\nu P_L \frac{1}{m_b \not{v} - \not{q} + i\not{D} - m_c} \gamma^\mu P_L b \\ &= \frac{1}{\Delta_0} \bar{b} \gamma^\nu P_L (m_b \not{v} - \not{q} + i\not{D} + m_c) \sum_{n=0}^{\infty} \left(\frac{D^2 - 2(m_b v - q) \cdot iD - \frac{1}{2} g \sigma_{\alpha\beta} G^{\alpha\beta}}{\Delta_0} \right)^n \gamma^\mu P_L b, \end{aligned} \quad (4.7)$$

where $P_L = \frac{1}{2}(1 - \gamma_5)$ is the left-handed projector, $\Delta_0 = (m_b v - q)^2 - m_c^2 + i0$, D is the covariant derivative, and $D_\mu D_\nu - D_\nu D_\mu = -ig G_{\mu\nu}$ was used. The field $b(x)$ in

Eq. (4.7) is related to the normal QCD field by $b_{\text{QCD}}(x) = e^{-im_b v \cdot x} b(x)$. There are other contributions in the OPE of two currents, e.g., the one in Fig. 4.1b. However these operators do not contribute to the decay rate once sandwiched between the B -meson states. For the diagram in Fig. 4.1b this is ensured by m_c being much larger than the available energy in the “brown muck,” which is of order Λ_{QCD} .

Our calculation of the form factors T_i follows the method of Ref. [41]. We expand Eq. (4.7) to third order in D . The term with no derivatives is proportional to the conserved current $\bar{b}\gamma_\mu b$, and thus its diagonal matrix elements can be evaluated exactly in full QCD. The corresponding contributions to the form factors are

$$\begin{aligned} T_1^{(0)} &= \frac{m_b - q \cdot v}{2\Delta_0}, \\ T_2^{(0)} &= \frac{m_b}{\Delta_0}, \\ T_3^{(0)} &= \frac{1}{2\Delta_0}, \\ T_4^{(0)} &= 0, \\ T_5^{(0)} &= -\frac{1}{2\Delta_0}. \end{aligned} \tag{4.8}$$

All other contributions we express in terms of the field h_v in the effective theory and reexpand the resulting expressions in powers of $1/m_b$. Therefore the expression for $b(x)$ in terms of $h_v(x)$ is needed to order $1/m_b^2$:

$$b(x) = \left(1 + \frac{i\not{D}_\perp}{2m_b} + \frac{(v \cdot D)\not{D}_\perp}{4m_b^2} - \frac{\not{D}_\perp^2}{8m_b^2} + \dots \right) h_v(x), \tag{4.9}$$

where $D_\perp = D - v(v \cdot D)$.

To evaluate the expectation values of the heavy quark bilinears we need the equations of motion in the effective theory to order $1/m_b^2$. They can be easily derived from Eq. (2.3):

$$iv \cdot D h_v = \left(\frac{1}{2m_b} \not{D}_\perp^2 - \frac{i}{4m_b^2} \not{D}_\perp (v \cdot D) \not{D}_\perp + \frac{i}{8m_b^2} \left(\not{D}_\perp^2 (v \cdot D) + (v \cdot D) \not{D}_\perp^2 \right) + \dots \right) h_v. \tag{4.10}$$

By virtue of Eq. (4.10) there are no nonperturbative corrections to the form factors

T_i at order $1/m_b$ [20]. The contributions at order $1/m_b^2$ can be expressed in terms of the matrix elements

$$\begin{aligned} K_B &= -\frac{1}{2m_b^2} \langle B(v) | \bar{h}_v (iD_\perp)^2 h_v | B(v) \rangle, \\ G_B &= -\frac{1}{2m_b^2} \langle B(v) | \bar{h}_v \frac{g}{2} \sigma_{\mu\nu} G^{\mu\nu} h_v | B(v) \rangle. \end{aligned} \quad (4.11)$$

Our calculation of these contributions reproduces the results in Ref. [41]:

$$\begin{aligned} T_1^{(2)} &= \frac{1}{6\Delta_0} m_b (K_B + G_B) + \frac{m_b}{3\Delta_0^2} K_B (3m_b q \cdot v + 2q^2 - 5(q \cdot v)^2) \\ &\quad + \frac{m_b}{3\Delta_0^2} G_B (7m_b q \cdot v + 2q^2 - 5(q \cdot v)^2 - 4m_b^2) \\ &\quad + \frac{4m_b^2}{3\Delta_0^3} K_B (m_b - q \cdot v) ((q \cdot v)^2 - q^2), \\ T_2^{(2)} &= \frac{5m_b}{3\Delta_0} (K_B + G_B) + \frac{14m_b^2}{3\Delta_0^2} q \cdot v K_B - \frac{2m_b^2}{3\Delta_0^2} (2m_b - 5q \cdot v) G_B \\ &\quad + \frac{8m_b^3}{3\Delta_0^3} ((q \cdot v)^2 - q^2) K_B, \\ T_3^{(2)} &= \frac{5m_b}{3\Delta_0^2} q \cdot v K_B - \frac{m_b}{3\Delta_0^2} (6m_b - 5q \cdot v) G_B + \frac{4m_b^2}{3\Delta_0^3} ((q \cdot v)^2 - q^2) K_B, \\ T_4^{(2)} &= \frac{4m_b}{3\Delta_0^2} (K_B + G_B), \\ T_5^{(2)} &= -\frac{m_b}{3\Delta_0^2} K_B (4m_b + 5q \cdot v) - \frac{5m_b}{3\Delta_0^2} q \cdot v G_B + \frac{4m_b^2}{3\Delta_0^3} (q^2 - (q \cdot v)^2) K_B. \end{aligned} \quad (4.13)$$

The states in the matrix elements Eqs. (4.11) have an implicit dependence on m_b . At order $1/m_b^2$ this dependence can be neglected, in which case K_B and G_B may be replaced by $-\lambda_1/(2m_b^2)$ and $-3\lambda_2/(2m_b^2)$ respectively. If the form factors are to be calculated to order $1/m_b^3$, then this replacement is no longer valid. An expression for the matrix elements Eq. (4.11) in terms of $\lambda_{1,2}$ and the expectation values of nonlocal operators is given below.

The $1/m_b^3$ contributions to the form factors T_i from local dimension-six operators can be parametrized by two matrix elements, ρ_1 and ρ_2 [45], defined in Eqs. (2.12). The expectation value of any bilinear operator with three derivatives is expressible in

terms of ρ_1 and ρ_2 :

$$\begin{aligned} \langle H_\infty(v) | \bar{h}_\nu \Gamma(iD_\alpha)(iD_\mu)(iD_\beta) h_\nu | H_\infty(v) \rangle = & \quad (4.14) \\ \frac{1}{6} \rho_1 (g_{\alpha\beta} - v_\alpha v_\beta) v_\mu \text{Tr} [P_+ \Gamma] - \frac{1}{12} d_H \rho_2 i \epsilon_{\nu\alpha\beta\delta} v^\nu v_\mu \text{Tr} [P_+ \gamma^\delta \gamma_5 P_+ \Gamma], & \end{aligned}$$

where $P_+ = \frac{1}{2}(1 + \not{v})$, and Γ is any four-by-four matrix.

After a rather lengthy calculation we obtain the contributions from local dimension-six operators to the form factors:

$$\begin{aligned} T_1^{(3)} = & -\frac{\rho_1 + 3\rho_2}{12\Delta_0 m_b^2} + \frac{1}{\Delta_0^2} \left[\frac{\rho_1}{3} - \rho_2 + \frac{(\rho_1 + 3\rho_2)(q^2 - q \cdot v^2 + m_b q \cdot v)}{6m_b^2} \right] \quad (4.15) \\ & + \frac{2(\rho_1 + 3\rho_2)}{3\Delta_0^3 m_b} (m_b - q \cdot v) (q^2 - q \cdot v^2) - \frac{4\rho_1}{3\Delta_0^4} (m_b - q \cdot v)^2 (q^2 - q \cdot v^2), \end{aligned}$$

$$\begin{aligned} T_2^{(3)} = & \frac{\rho_1 + 3\rho_2}{6\Delta_0 m_b^2} + \frac{1}{3\Delta_0^2} \left[4\rho_1 + 6\rho_2 - (\rho_1 + 3\rho_2) \frac{q \cdot v}{m_b} \right] \quad (4.16) \\ & + \frac{2}{3\Delta_0^3} \left[(4\rho_1 + 6\rho_2)(m_b - q \cdot v) q \cdot v - 3\rho_2 q^2 \right] - \frac{8m_b \rho_1}{3\Delta_0^4} (m_b - q \cdot v) (q^2 - q \cdot v^2), \end{aligned}$$

$$\begin{aligned} T_3^{(3)} = & \frac{\rho_1 + 3\rho_2}{6m_b^2 \Delta_0^2} q \cdot v + \frac{2(m_b - q \cdot v)}{3\Delta_0^3} \left[(\rho_1 + 3\rho_2) \frac{q \cdot v}{m_b} - 3\rho_2 \right] \\ & - \frac{4\rho_1}{3\Delta_0^4} (m_b - q \cdot v) (q^2 - q \cdot v^2), \quad (4.17) \end{aligned}$$

$$T_4^{(3)} = \frac{\rho_1 + 3\rho_2}{3m_b^2 \Delta_0^2} - \frac{2\rho_2}{\Delta_0^3} + \frac{4(\rho_1 + 3\rho_2)}{3m_b \Delta_0^3} (m_b - q \cdot v), \quad (4.18)$$

$$\begin{aligned} T_5^{(3)} = & -\frac{\rho_1 + 3\rho_2}{6m_b^2 \Delta_0^2} q \cdot v - \frac{2(\rho_1 + 3\rho_2)}{3m_b \Delta_0^3} q \cdot v (m_b - q \cdot v) + \frac{2\rho_2 m_b}{\Delta_0^3} \\ & + \frac{4\rho_1}{3\Delta_0^4} (m_b - q \cdot v) (q^2 - q \cdot v^2). \quad (4.19) \end{aligned}$$

Substituting the imaginary part of these form factors into Eq. (4.4) we obtain the triple differential decay rate. Interesting quantities are the charged lepton spectrum

and the hadronic spectrum. The former is obtained by integrating Eq. (4.4) over q^2 and E_ν . Using the rescaled lepton energy $y = 2E_\ell/m_b$ we find the lepton spectrum

$$\frac{d\Gamma}{dy} = \frac{d\Gamma^{(0)}}{dy} + \frac{d\Gamma^{(2)}}{dy} + \frac{d\Gamma^{(3)}}{dy}, \quad (4.20)$$

where

$$\frac{d\Gamma^{(0)}}{dy} = \Gamma_0 \theta(1-r-y) \left[2(3-2y)y^2 - 6y^2r - \frac{6y^2r^2}{(1-y)^2} + \frac{2(3-y)y^2r^3}{(1-y)^3} \right], \quad (4.21)$$

$$\begin{aligned} \frac{d\Gamma^{(2)}}{dy} = & \Gamma_0 \left\{ K_B \left[-\frac{20y^3}{3} - \frac{4r^2y^3(5-7y+2y^2)}{(1-y)^5} + \frac{8r^3y^3(10-5y+y^2)}{3(1-y)^5} \right] \right. \\ & + G_B \left[\frac{4y^2(6-5y)}{3} + \frac{8ry^2(3-2y)}{(1-y)^2} + \frac{12r^2y^2(2-y)}{(1-y)^3} \right. \\ & \left. \left. - \frac{20y^2(6-4y+y^2)}{3(1-y)^4} \right] \right\} \theta(1-r-y) \end{aligned} \quad (4.22)$$

$$\begin{aligned} \frac{d\Gamma^{(3)}}{dy} = & \frac{\Gamma_0}{m_b^3} \left\{ \left[\frac{8}{3} (3\rho_1 + r^2\rho_1 + 9r^2\rho_2 - 3r^3\rho_2) + \frac{8}{3}\rho_1y(3-2r) - 8\rho_1y^2 \right. \right. \\ & - \frac{2}{3}(\rho_1 + 3\rho_2)y^3 - \frac{2(4\rho_1 + 3r^2\rho_1 + 9r^2\rho_2)}{1-y} - \frac{2r(8\rho_1 + 9r\rho_1 + 27r\rho_2)}{3(1-y)^2} \\ & + \frac{2r(8\rho_1 + 17r\rho_1 + 4r^2\rho_1 - 9r\rho_2 + 12r^2\rho_2)}{3(1-y)^3} + \frac{2r^2(3+4r)(\rho_1 + 3\rho_2)}{(1-y)^4} \\ & \left. - \frac{8r^2(\rho_1 + 3r\rho_1 + 3r\rho_2)}{(1-y)^5} + \frac{40r^3\rho_1}{3(1-y)^6} \right] \theta(1-r-y) \\ & \left. - \frac{2(1-r)^4(1+r)^2\rho_1}{3r^2} \delta(1-r-y) \right\}. \end{aligned} \quad (4.23)$$

Here $r = (m_c/m_b)^2$. Note the contribution from the δ -function at the end point of the lepton spectrum. For $b \rightarrow u$ transition such singular terms in the lepton spectrum appear already at order $1/m_b^2$, but for $b \rightarrow c$ they do not appear until order $1/m_b^3$. This is easily explained if one recalls that the most singular contributions to the lepton spectrum at a given order $1/m_b^n$ can be obtained from the spectator model result by the ‘‘averaging’’ procedure of Ref. [41], which involves differentiating n times with

respect to y . For a massless final state quark the spectator model spectrum has the form $f(y)\theta(1-y)$ with $f(1) \neq 0$, and thus differentiation produces the $n-1$ -st derivative of the δ -function $\delta^{(n-1)}(1-y)$. For a massive quark in the final state the spectator model spectrum and its first derivative vanish at the end point $y = 1-r$. Hence at order $1/m_b^n$ the most singular contribution is proportional to $\delta^{(n-3)}(1-y-r)$.

To obtain the hadronic spectrum we integrate Eq. (4.4) over E_ν and express the result in terms of rescaled hadronic variables $\hat{E}_0 = (m_b - q \cdot v)/m_b$ and $\hat{s}_0 = (m_b^2 - 2q \cdot v + q^2)/m_b^2$. This yields

$$\frac{d\Gamma}{d\hat{s}_0 d\hat{E}_0} = \frac{d\Gamma^{(0)}}{d\hat{s}_0 d\hat{E}_0} + \frac{d\Gamma^{(2)}}{d\hat{s}_0 d\hat{E}_0} + \frac{d\Gamma^{(3)}}{d\hat{s}_0 d\hat{E}_0}, \quad (4.24)$$

where

$$\begin{aligned} \frac{d\Gamma^{(0)}}{d\hat{s}_0 d\hat{E}_0} &= 32\Gamma_0 \theta(\hat{E}_0 - \sqrt{\hat{s}_0}) \theta(1 + \hat{s}_0 - 2\hat{E}_0) \sqrt{\hat{E}_0^2 - \hat{s}_0} \delta(\hat{s}_0 - r) \times \\ &\quad \left[(1 - 2\hat{E}_0 + \hat{s}_0) \frac{3\hat{E}_0}{2} + \hat{E}_0^2 - \hat{s}_0 \right], \end{aligned} \quad (4.25)$$

$$\begin{aligned} \frac{d\Gamma^{(2)}}{d\hat{s}_0 d\hat{E}_0} &= 32\Gamma_0 \theta(\hat{E}_0 - \sqrt{\hat{s}_0}) \theta(1 + \hat{s}_0 - 2\hat{E}_0) \sqrt{\hat{E}_0^2 - \hat{s}_0} \times \\ &\quad \left\{ \delta(\hat{s}_0 - r) (K_B + G_B) \left[\frac{1}{2}(1 - 2\hat{E}_0 + \hat{s}_0) + \frac{5}{3}(\hat{E}_0^2 - \hat{s}_0) \right] \right. \\ &\quad + \delta'(\hat{s}_0 - r) \left[(1 - 2\hat{E}_0 + \hat{s}_0) (K_B(5\hat{E}_0^2 - 3\hat{E}_0 - 2\hat{s}_0) + G_B(5\hat{E}_0^2 + \hat{E}_0 - 2\hat{s}_0)) \right. \\ &\quad \left. \left. + (\hat{E}_0^2 - \hat{s}_0) \left(\frac{14}{3}K_B(\hat{E}_0 - 1) + \frac{2}{3}G_B(5\hat{E}_0 - 3) \right) \right] \right. \\ &\quad \left. + \delta''(\hat{s}_0 - r) K_B(\hat{E}_0^2 - \hat{s}_0) \left[2(1 - 2\hat{E}_0 + \hat{s}_0)\hat{E}_0 + \frac{4}{3}(\hat{E}_0^2 - \hat{s}_0) \right] \right\}, \end{aligned} \quad (4.26)$$

$$\begin{aligned} \frac{d\Gamma^{(3)}}{d\hat{s}_0 d\hat{E}_0} &= \frac{8\Gamma_0}{3m_b^3} \theta(\hat{E}_0 - \sqrt{\hat{s}_0}) \theta(1 + \hat{s}_0 - 2\hat{E}_0) \sqrt{\hat{E}_0^2 - \hat{s}_0} \times \\ &\quad \left\{ (\rho_1 + 3\rho_2)(-3 + 6\hat{E}_0 + 2\hat{E}_0^2 - 5\hat{s}_0) \delta(\hat{s}_0 - r) - 2[9(\rho_1 - \rho_2) \right. \\ &\quad \left. + 6(\rho_1 - \rho_2)\hat{s}_0 + 3(\rho_1 + 3\rho_2)\hat{s}_0^2 - (3(7\rho_1 - 3\rho_2) + 11(\rho_1 + 3\rho_2)\hat{s}_0)\hat{E}_0 \right. \end{aligned} \quad (4.27)$$

$$\begin{aligned}
& + 3((3\rho_1 + 5\rho_2) - (\rho_1 + 3\rho_2)\hat{s}_0)\hat{E}_0^2 + 8(\rho_1 + 3\rho_2)\hat{E}_0^3] \delta'(\hat{s}_0 - r) \\
& - 4(\hat{E}_0^2 - \hat{s}_0) \left[3(1 + \hat{s}_0)\rho_2 - (1 - 3\hat{s}_0)(\rho_1 + 3\rho_2)\hat{E}_0 - 2(\rho_1 + 6\rho_2)\hat{E}_0^2 \right] \delta''(\hat{s}_0 - r) \\
& + \frac{8}{3}\hat{E}_0(\hat{E}_0^2 - \hat{s}_0)\rho_1 \left[2\hat{s}_0 - 3(1 + \hat{s}_0)\hat{E}_0 + 4\hat{E}_0^2 \right] \delta'''(\hat{s}_0 - r) \Big\}.
\end{aligned}$$

The total rate is given by integrating Eq. (4.20) or Eq. (4.24) over the remaining variables:

$$\Gamma = \Gamma^{(0)} + \Gamma^{(2)} + \Gamma^{(3)}, \quad (4.28)$$

where

$$\Gamma^{(0)} = \Gamma_0 \left[1 - 8r + 8r^3 - r^4 - 12r^2 \log r \right], \quad (4.29)$$

$$\begin{aligned}
\Gamma^{(2)} = \Gamma_0 & \left[K_B(-1 + 8r - 8r^3 + r^4 + 12r^2 \log r) \right. \\
& \left. + G_B(3 - 8r + 24r^2 - 24r^3 + 5r^4 + 12r^2 \log r) \right], \quad (4.30)
\end{aligned}$$

$$\begin{aligned}
\Gamma^{(3)} = \frac{\Gamma_0}{6m_b^3} & \left[\rho_1(77 - 88r + 24r^2 - 8r^3 - 5r^4 + 48 \log r + 36r^2 \log r) \right. \\
& \left. + \rho_2(27 - 72r + 216r^2 - 216r^3 + 45r^4 + 108r^2 \log r) \right]. \quad (4.31)
\end{aligned}$$

The part of Eq. (4.31) that diverges logarithmically as $r \rightarrow 0$ agrees with the corresponding expression in Ref. [46]. There is nothing wrong with the logarithmic divergence, since our calculation is valid only for the charm mass significantly larger than Λ_{QCD} . It is the latter condition that allowed us to discard the diagram in Fig. 1b.

Above we have computed the $1/m_b^3$ corrections to the inclusive differential B decay rate from the local dimension-six operators in the OPE. However, there are other sources of $1/m_b^3$ corrections. At order $1/m_b^2$ the OPE yields the decay rate in terms of the two matrix elements K_B and G_B defined in Eqs. (4.11). The state $|B(v)\rangle$ in Eqs. (4.11) is the physical B -meson state, rather than the state of the effective theory in the infinite mass limit $|B_\infty(v)\rangle$. Thus K_B and G_B are mass-dependent. At order $1/m_b^2$ this distinction is irrelevant, but at higher orders this mass dependence has to be taken into account explicitly. We express the physical states through the states

in the infinite mass limit of HQET using the Gell-Mann and Low theorem (see e.g., Ref. [12]). This theorem implies that, to first order in $1/m_b$, $|B(v)\rangle$ is given by

$$|B(v)\rangle = \frac{1}{V} \left[1 + i \int d^3x \int_{-\infty}^0 dt \mathcal{L}_I(x) - \frac{1}{V} \langle B_\infty(v) | i \int d^3x \int_{-\infty}^0 dt \mathcal{L}_I(x) | B_\infty(v) \rangle \right] |B_\infty(v)\rangle, \quad (4.32)$$

where V is the normalization volume and

$$\mathcal{L}_I = \frac{1}{2m_b} \bar{h}_v (iD_\perp)^2 h_v + \frac{1}{2m_b} \bar{h}_v \frac{g}{2} \sigma_{\mu\nu} G^{\mu\nu} h_v. \quad (4.33)$$

Using Eq. (4.32), one can easily expand K_B and G_B to order $1/m_b^3$. The result can be presented in terms of λ_1, λ_2 and matrix elements $\mathcal{T}_1 - \mathcal{T}_4$ defined in Eqs. (2.13):

$$\begin{aligned} K_B &= -\frac{\lambda_1}{2m_b^2} - \frac{\mathcal{T}_1 + 3\mathcal{T}_2}{2m_b^3}, \\ G_B &= -\frac{3\lambda_2}{2m_b^2} - \frac{\mathcal{T}_3 + 3\mathcal{T}_4}{2m_b^3}. \end{aligned} \quad (4.34)$$

Turning now to corrections suppressed by powers of α_s (but not by powers of $1/m_b$), we note that they may be computed using the free quark decay (or parton) model. Order α_s corrections to the lepton spectrum have been computed in Ref. [39], while the corrections to the moments of the hadron energy and invariant mass spectrum can be found in Ref. [40]. In Ref. [47] the (supposedly) leading part of the α_s^2 corrections to the lepton spectrum has been computed. The formulae are messy, and we will not list them here.

4.2 Applications

“If your Snark be a Snark, that is right:

Fetch it home by all means—you may serve it with greens,

And it’s handy for striking a light.”

Lewis Carroll [1]

One important application of the results of the previous section is the extraction of the HQET matrix elements $\bar{\Lambda}, \lambda_1$ from the shape of the charged lepton spectrum in $B \rightarrow X_c \ell \bar{\nu}_\ell$ decays [35, 11]. The CLEO Collaboration has measured the inclusive $B \rightarrow X \ell \bar{\nu}_\ell$ lepton spectrum both by demanding only one charged lepton tag [43], and using a double tagged data sample [44] where the charge of a high momentum lepton determines whether the other lepton in the event comes directly from semileptonic B decay (primary) or from the semileptonic decay of a B decay product charmed hadron (secondary). The single tagged data sample has smaller statistical errors, but it is significantly contaminated by secondary leptons below about 1.5 GeV. For our analysis we use the data as tabulated in Ref. [48].

The OPE for the lepton spectrum in semileptonic B decay does not reproduce the physical lepton spectrum point-by-point near the maximal lepton energy. Near the end point, a comparison with experimental data can only be made after sufficient smearing, or after integrating over a sufficiently large region. The minimal size of this region was estimated to be around 300 – 500 MeV [41]. This, and the fact that the experimental measurement of the lepton spectrum is precise and model independent only above about 1.5 GeV, impose a limitation on what quantities can be reliably predicted and compared with data. On the one hand, we want to find observables sensitive to $\bar{\Lambda}$ and λ_1 ; on the other hand, we want the deviations from the b quark decay prediction to be small, so that the contributions from even higher dimension operators in the OPE are not too important. The observables we use should not depend on $|V_{cb}|$. Thus we consider

$$R_1 = \frac{\int_{1.5 \text{ GeV}} E_\ell \frac{d\Gamma}{dE_\ell} dE_\ell}{\int_{1.5 \text{ GeV}} \frac{d\Gamma}{dE_\ell} dE_\ell}, \quad R_2 = \frac{\int_{1.7 \text{ GeV}} \frac{d\Gamma}{dE_\ell} dE_\ell}{\int_{1.5 \text{ GeV}} \frac{d\Gamma}{dE_\ell} dE_\ell}. \quad (4.35)$$

Before comparing the experimental data with the theoretical predictions for $R_{1,2}$, derived from the OPE and QCD perturbation theory, the following corrections have to be included: (i) electromagnetic radiative correction; (ii) effects of a boost into the lab frame; (iii) smearing due to the detector momentum resolution. To take (i)

into account, following the CLEO analysis, we used the resummed photon radiation corrections as given in Ref. [49]. These corrections to $R_{1,2}$ have very little sensitivity to subleading logarithms. To determine the corrections due to (ii), we assume that the B mesons are monoenergetic, with energy $m_{\Upsilon(4S)}/2$ (the effect of the 4 MeV spread in the center of mass energy is negligible). We found that the smearing due to the CLEO-II detector momentum resolution [50], and the 50 MeV binning of the data has a negligible effect on $R_{1,2}$.

Including the nonperturbative corrections of order $(\Lambda_{\text{QCD}}/m_b)^2$ and $(\Lambda_{\text{QCD}}/m_b)^3$ computed above and the order α_s corrections, the theoretical expressions for $R_{1,2}$ are

$$\begin{aligned}
R_1[\text{GeV}] = & 1.8059 - 0.309 \frac{\bar{\Lambda}}{\bar{m}_B} - 0.35 \frac{\bar{\Lambda}^2}{\bar{m}_B^2} - 2.32 \frac{\lambda_1}{\bar{m}_B^2} - 3.96 \frac{\lambda_2}{\bar{m}_B^2} - 0.4 \frac{\bar{\Lambda}^3}{\bar{m}_B^3} - 5.7 \frac{\bar{\Lambda}\lambda_1}{\bar{m}_B^3} \\
& - 6.8 \frac{\bar{\Lambda}\lambda_2}{\bar{m}_B^3} - 7.7 \frac{\rho_1}{\bar{m}_B^3} - 1.3 \frac{\rho_2}{\bar{m}_B^3} - 3.2 \frac{\mathcal{T}_1}{\bar{m}_B^3} - 4.5 \frac{\mathcal{T}_2}{\bar{m}_B^3} - 3.1 \frac{\mathcal{T}_3}{\bar{m}_B^3} - 4.0 \frac{\mathcal{T}_4}{\bar{m}_B^3} \\
& - \frac{\alpha_s}{\pi} \left(0.035 + 0.07 \frac{\bar{\Lambda}}{\bar{m}_B} \right) + \left| \frac{V_{ub}}{V_{cb}} \right|^2 \left(1.33 - 10.3 \frac{\bar{\Lambda}}{\bar{m}_B} \right) \\
& - \left(0.0041 - 0.004 \frac{\bar{\Lambda}}{\bar{m}_B} \right) + \left(0.0062 + 0.002 \frac{\bar{\Lambda}}{\bar{m}_B} \right), \tag{4.36}
\end{aligned}$$

$$\begin{aligned}
R_2 = & 0.6581 - 0.315 \frac{\bar{\Lambda}}{\bar{m}_B} - 0.68 \frac{\bar{\Lambda}^2}{\bar{m}_B^2} - 1.65 \frac{\lambda_1}{\bar{m}_B^2} - 4.94 \frac{\lambda_2}{\bar{m}_B^2} - 1.5 \frac{\bar{\Lambda}^3}{\bar{m}_B^3} - 7.1 \frac{\bar{\Lambda}\lambda_1}{\bar{m}_B^3} \\
& - 17.5 \frac{\bar{\Lambda}\lambda_2}{\bar{m}_B^3} - 1.8 \frac{\rho_1}{\bar{m}_B^3} + 2.3 \frac{\rho_2}{\bar{m}_B^3} - 2.9 \frac{\mathcal{T}_1}{\bar{m}_B^3} - 1.5 \frac{\mathcal{T}_2}{\bar{m}_B^3} - 4.0 \frac{\mathcal{T}_3}{\bar{m}_B^3} - 4.9 \frac{\mathcal{T}_4}{\bar{m}_B^3} \\
& - \frac{\alpha_s}{\pi} \left(0.039 + 0.18 \frac{\bar{\Lambda}}{\bar{m}_B} \right) + \left| \frac{V_{ub}}{V_{cb}} \right|^2 \left(0.87 - 3.8 \frac{\bar{\Lambda}}{\bar{m}_B} \right) \\
& - \left(0.0073 + 0.005 \frac{\bar{\Lambda}}{\bar{m}_B} \right) + \left(0.0021 + 0.003 \frac{\bar{\Lambda}}{\bar{m}_B} \right), \tag{4.37}
\end{aligned}$$

where the first two lines contain the nonperturbative corrections to order $1/\bar{m}_B^3$. The other terms are in order: the perturbative α_s corrections, the contribution from $B \rightarrow X_u \ell \nu$ decays, electroweak corrections, and finally a boost, since the B -mesons do not decay from rest. The spin-averaged heavy meson masses are defined as $\bar{m}_B = (m_B + 3m_{B^*})/4$, $\bar{m}_D = (m_D + 3m_{D^*})/4$. Even though there are no nonperturbative corrections to $R_{1,2}$ of order Λ_{QCD}/m_b , Eqs. (4.36,4.37) contain terms proportional to

$\bar{\Lambda}/\bar{m}_B$. These arise since we reexpressed the heavy quark masses in terms of hadron masses using Eq. (2.14).

Eqs. (4.36,4.37) correspond to electrons; for muons the electromagnetic correction is smaller. Namely, the electromagnetic corrections to R_1, R_2 for muons are

$$\begin{aligned}\delta R_1[\text{GeV}] &= - \left(0.0014 - 0.001 \frac{\bar{\Lambda}}{\bar{m}_B} \right), \\ \delta R_2 &= - \left(0.0025 + 0.002 \frac{\bar{\Lambda}}{\bar{m}_B} \right).\end{aligned}\tag{4.38}$$

To compare the above theoretical expressions with data, we need to discuss the experimental uncertainties. We use the single tagged data to extract $R_{1,2}$, and correct for the effects of secondary leptons using the double tagged data. The central values are $R_1 = 1.7831$ GeV and $R_2 = 0.6159$ (including the corrections from the secondaries which are 0.0001 GeV and 0.0051, respectively), while the correlation matrix of the statistical errors [48] is

$$V(R_1, R_2) = \begin{pmatrix} 3.8 \times 10^{-6} & 6.0 \times 10^{-6} \\ 6.0 \times 10^{-6} & 1.7 \times 10^{-5} \end{pmatrix}.\tag{4.39}$$

The largest part of these uncertainties is due to the errors in the secondary lepton spectrum from the double tagged data. Estimating the systematic errors is more complicated. These uncertainties in the lepton spectrum can be divided into two classes: there are additive corrections, like backgrounds that are subtracted from the data; and there are multiplicative corrections, like those in efficiencies. The total systematic uncertainty in the CLEO measurement of the semileptonic B decay branching fraction is about 2%. However, only a small fraction of these uncertainties affect the shape of the lepton spectrum above 1.5 GeV [51]. In this region the uncertainties in the backgrounds are small, and the efficiencies have fairly flat momentum dependences. While the uncertainties in the electron identification and in the tracking efficiencies are the dominant sources of systematic error in the semileptonic B branching fraction, they are expected to affect $R_{1,2}$ at a much smaller level. We estimate that the systematic uncertainties in $R_{1,2}$ are not larger than the statistical errors [51], although

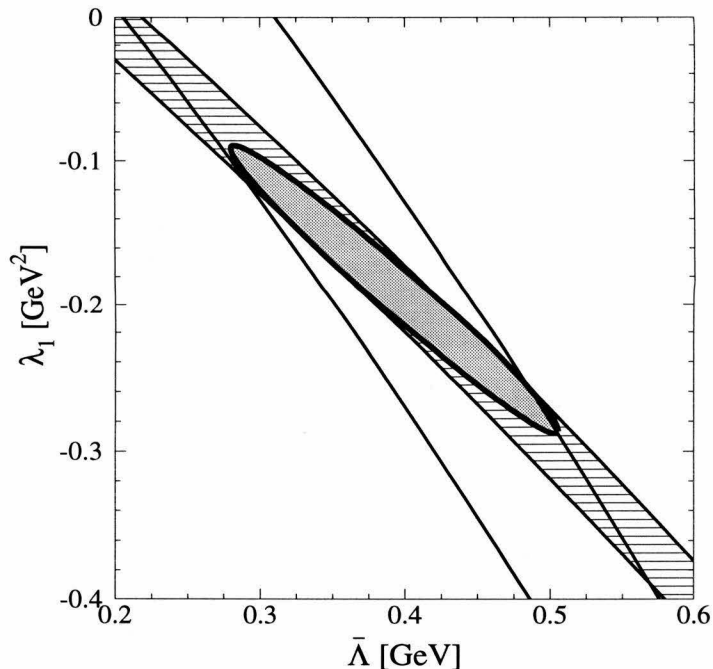


Figure 4.2: Allowed regions in the $\bar{\Lambda} - \lambda_1$ plane for R_1 and R_2 with $1/m_b^3$ corrections omitted. The bands represent the 1σ statistical errors, while the ellipse is the allowed region taking correlations into account.

a complete analysis of these can only be carried out by the CLEO Collaboration. For this reason, and since the statistical errors can be included into our analysis exactly, the experimental uncertainties we shall quote will be the statistical ones only.

To extract λ_1 and $\bar{\Lambda}$, we first set all order $1/m_b^3$ contributions in Eqs. (4.36,4.37) to zero. We also set $|V_{ub}/V_{cb}| = 0.08, \alpha_s = 0.22, \lambda_2 = 0.12 \text{ GeV}^2$. The comparison of the resulting theoretical predictions in Eqs. (4.36,4.37) with the CLEO data is shown in Fig. 4.2. The steeper band is the constraint from R_2 , while the hatched one is that from R_1 . The widths of the bands represent the 1σ statistical errors, while the ellipse shows the 1σ allowed region in $\{\bar{\Lambda}, \lambda_1\}$, after correlations between R_1 and R_2 are taken into account. This region corresponds to $\bar{\Lambda} = 0.39 \pm 0.11 \text{ GeV}$ and $\lambda_1 = -0.19 \pm 0.10 \text{ GeV}^2$.

The value of $|V_{ub}/V_{cb}|$ has considerable uncertainty. If $|V_{ub}/V_{cb}| = 0.1$ then the

center of the ellipse in Fig. 4.2 would move to $\bar{\Lambda} = 0.42 \text{ GeV}$ and $\lambda_1 = -0.19 \text{ GeV}^2$. We used $\alpha_s = 0.22$, $\lambda_2 = 0.12 \text{ GeV}^2$, corresponding to the subtraction scale m_b . The sensitivity of our results to this choice of scale is weak: changing α_s to 0.35 moves the central values to $\bar{\Lambda} = 0.36 \text{ GeV}$ and $\lambda_1 = -0.18 \text{ GeV}^2$.

To plot Fig. 4.2 we used the data corresponding to electrons only, as we suspect that the systematic uncertainties in the (single tagged) muon data may be larger (for example, the muon detection efficiency is strongly energy dependent below 2 GeV). The latter data set, nevertheless, yields a consistent determination of $\bar{\Lambda}$ and λ_1 , giving central values $\bar{\Lambda} = 0.43 \text{ GeV}$ and $\lambda_1 = -0.21 \text{ GeV}^2$ (to subtract secondaries we used the double tagged electron data).

Theoretical uncertainties in our determination of $\bar{\Lambda}$ and λ_1 originate from the reliability of quark-hadron duality at the scales corresponding to the limits in the integrals defining $R_{1,2}$, from order $(\Lambda_{\text{QCD}}/m_b)^3$ corrections, and from higher order perturbative corrections. Concerning duality, note that $E_\ell \geq 1.5 \text{ GeV}$ and 1.7 GeV (in the lab frame) correspond to summing over hadronic states X with masses below 3.6 GeV and 3.3 GeV , respectively. These scales are likely to be large enough to trust the OPE locally. This is supported by the fact that a modified ratio that differs from R_2 only in that the integration limit in the numerator is changed from 1.7 GeV to 1.8 GeV yields a parallel band that overlaps with that corresponding to R_2 . Using this variable and R_1 , the central values for $\bar{\Lambda}$ and λ_1 become $\bar{\Lambda} = 0.47 \text{ GeV}$ and $\lambda_1 = -0.26 \text{ GeV}^2$. (The assumption of local duality becomes less reliable using 1.8 GeV .) For higher moments theoretical uncertainties increase, and they are sensitive to an almost identical combination of $\bar{\Lambda}$ and λ_1 as the first moment, R_1 . For example, the normalized second moment (with $E_\ell > 1.5 \text{ GeV}$) gives a band that overlaps with that from R_1 , and together with R_2 yields the central values $\bar{\Lambda} = 0.39 \text{ GeV}$ and $\lambda_1 = -0.19 \text{ GeV}^2$. Perturbative corrections of order α_s^2 and order $\alpha_s(\Lambda_{\text{QCD}}/m_b)^2$ have not been computed. However, the computation of $\alpha_s^2\beta_0$ corrections has recently become available [47]. According to Ref. [47], taking into account terms of order $\alpha_s^2\beta_0$ shifts the extracted values of $\bar{\Lambda}$, λ_1 to $\bar{\Lambda} = 0.33 \text{ GeV}$, $\lambda_1 = -0.17 \text{ GeV}^2$. If we assume

that $\alpha_s^2\beta_0$ corrections dominate the full order α_s^2 corrections,² this implies that the latter do not introduce a significant uncertainty.

In order to take the uncertainties from the higher order matrix elements into account, we equate the expressions for $R_{1,2}$, Eqs. (4.36,4.37), to the experimental values using $|V_{ub}/V_{cb}| = 0.08, \alpha_s = 0.22$. The familiar relation of the HQET matrix element λ_2 to the mass splitting between B and B^* mesons has to be extended to include the $1/m_b^3$ contributions. Using Eq. (2.14) to express the quark mass through the meson mass and $\bar{\Lambda}$, we find

$$m_{H^*} - m_H = \Delta m_H = 2 \frac{\kappa(m_Q)\lambda_2(m_b)}{m_H} \left(1 + \frac{\bar{\Lambda}}{m_H}\right) - \frac{\rho_2}{m_H^2} + \frac{\mathcal{T}_2 + \mathcal{T}_4}{m_H^2}, \quad (4.40)$$

where $H = B$ or D , and $\kappa(m_Q) = (\alpha_s(m_Q)/\alpha_s(m_b))^{3/\beta_0}$ takes account of the scale dependence of λ_2 . We can use the $B - B^*$ and $D - D^*$ mass splittings $\Delta m_B, \Delta m_D$ to extract the numerical value of some of the HQET matrix elements:

$$\begin{aligned} \lambda_2(m_b) &= \frac{\Delta m_B m_B^2 - \Delta m_D m_D^2}{2(m_B - \kappa(m_c)m_D)}, \\ \rho_2 - \mathcal{T}_2 - \mathcal{T}_4 &= \frac{\kappa(m_c)m_B^2\Delta m_B(m_D + \bar{\Lambda}) - m_D^2\Delta m_D(m_B + \bar{\Lambda})}{m_B + \bar{\Lambda} - \kappa(m_c)(m_D + \bar{\Lambda})}. \end{aligned} \quad (4.41)$$

Eq. (4.41) yields $\lambda_2(m_b) = 0.120 \text{ GeV}^2$. Using Eqs. (4.41) to eliminate λ_2 and ρ_2 yields the extracted values of $\bar{\Lambda}, \lambda_1$ in the form

$$\bar{\Lambda} = f_{\bar{\Lambda}}(R_1^{exp}, R_2^{exp}, \rho_1, \mathcal{T}_1, \mathcal{T}_2, \mathcal{T}_3, \mathcal{T}_4), \quad \lambda_1 = f_{\lambda_1}(R_1^{exp}, R_2^{exp}, \rho_1, \mathcal{T}_1, \mathcal{T}_2, \mathcal{T}_3, \mathcal{T}_4). \quad (4.42)$$

Dimensional analysis suggests that the higher order matrix elements are all of order Λ_{QCD}^3 , which can be used to make a quantitative estimate of the uncertainties in the extraction of $\bar{\Lambda}, \lambda_1$. We vary the magnitude of $\rho_1, \mathcal{T}_1 - \mathcal{T}_4$ in Eqs. (4.42) independently in the range $0 - (0.5\text{GeV})^3$, taking ρ_1 to be positive, as indicated by the vacuum saturation approximation (see below), but making no assumption

²This assumption is supported by the results of Refs. [27, 52], where the full two-loop corrections to $d\Gamma/dq^2$ were computed both at maximum and zero q^2 . It turns out that in both cases order $\alpha_s^2\beta_0$ corrections provide a good approximation to the full result.

about the sign of the other matrix elements. Using the central values for $R_{1,2}^{exp}$ we find that $\bar{\Lambda}, \lambda_1$ can lie inside the shaded region in Fig. 4.3. This corresponds to $\bar{\Lambda} = 0.45 \pm 0.3 \text{ GeV}$, $\lambda_1 = -0.25 \pm 0.35 \text{ GeV}^2$. Clearly the theoretical uncertainties dominate the accuracy to which $\bar{\Lambda}, \lambda_1$ can be extracted.

The situation can be improved if we have some independent information on some or all of the higher dimension matrix elements. This requires either more experimental input or theoretical estimates of these matrix elements. ρ_1 can be estimated in the vacuum saturation approximation [53, 54, 9, 45, 55, 35], $\rho_1 = (2\pi\alpha_s/9)m_B f_B^2$. The numerical value obtained this way is rather uncertain. Taking $\alpha_s = 0.5$ and $f_B = 270 \text{ MeV}$ for purposes of illustration, we find $\rho_1 \simeq 0.13 \text{ GeV}^3$.³ No similar estimates exist for the other dimension-six matrix elements. ρ_2 vanishes in any non relativistic potential model, which may be taken as an indication that it is small relative to the other matrix elements. No estimates that go beyond dimensional analysis are available for the time ordered products.

The cross hatched region in Fig. 4.3 shows the range of $\bar{\Lambda}, \lambda_1$ one obtains from setting $\rho_1 = 0.13 \text{ GeV}^3$ and $\rho_2 = 0$ and varying the magnitude of the other matrix elements in the range $0 - (0.5 \text{ GeV})^3$. The previously extracted values of $\bar{\Lambda}, \lambda_1$ are not excluded by this choice of $\rho_{1,2}$.

Fig. 4.3 seems to suggest that $1/m_b^3$ corrections are anomalously large. However, this is not the case. Rather, this method of extracting $\bar{\Lambda}, \lambda_1$ is especially sensitive to higher order nonperturbative corrections because the constraints obtained from R_1 and R_2 give almost parallel bands in the $\bar{\Lambda} - \lambda_1$ plane. Thus small uncertainties in the theoretical expressions for $R_{1,2}$ result in large uncertainties in the extracted values of $\bar{\Lambda}, \lambda_1$. Put differently, Fig. 4.3 means that we are able to determine accurately one linear combination of $\bar{\Lambda}$ and λ_1 , while the orthogonal linear combination is only weakly constrained by the data. In the next chapter we will see that the rare decay $B \rightarrow X_s \gamma$ provides a way to extract a vertical band in the $\bar{\Lambda} - \lambda_1$ plane, but at present the experimental data does not allow a quantitative analysis.

³A value for ρ_1 can also be obtained from small velocity sum rules [55], but this estimate suffers from large uncertainties as well.

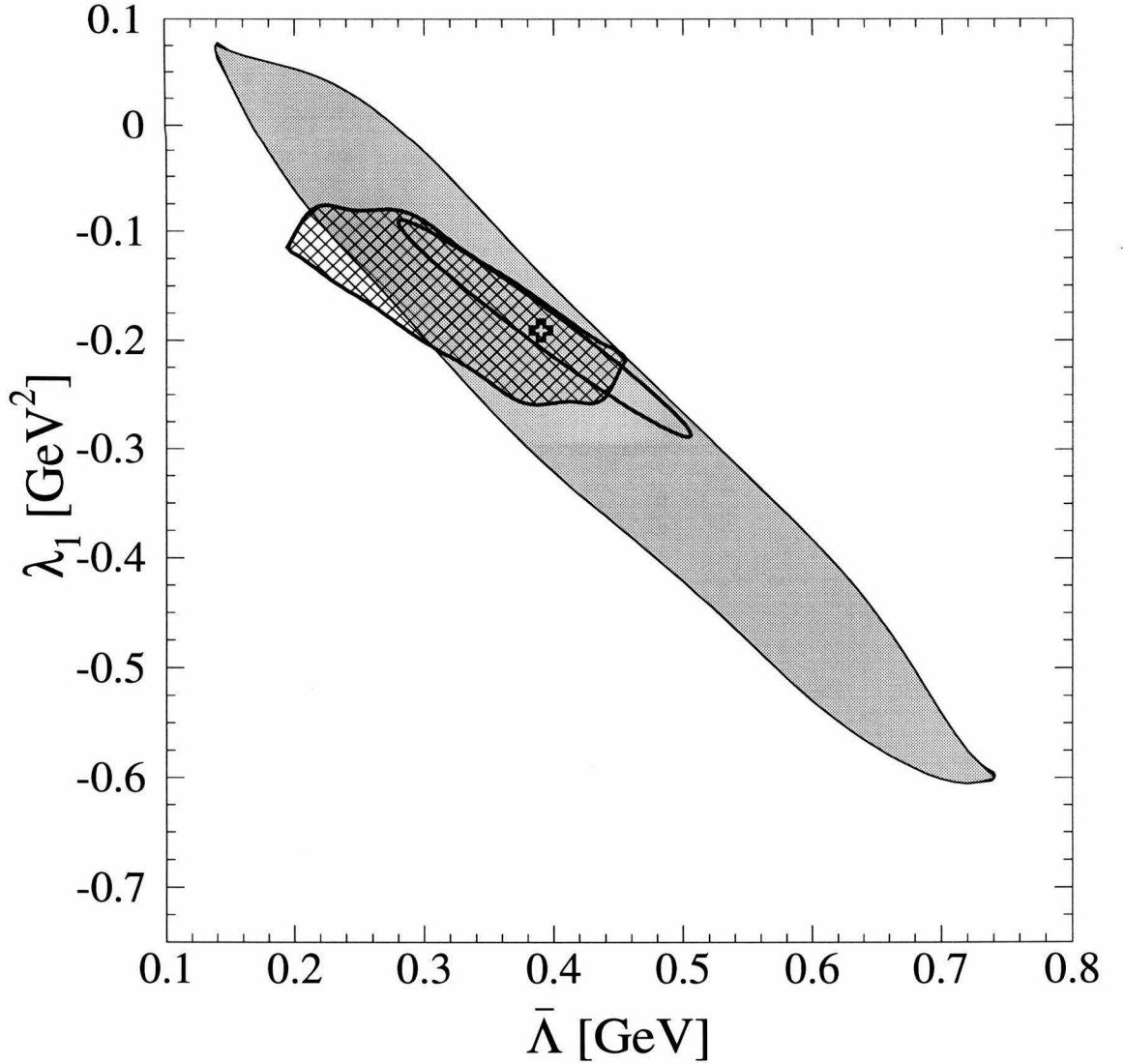


Figure 4.3: Extraction of $\bar{\Lambda}, \lambda_1$. Cross and ellipse show the values of $\bar{\Lambda}, \lambda_1$ extracted without $1/m_b^3$ corrections but including the experimental statistical error. Shaded region: Higher order matrix elements estimated by dimensional analysis. Cross-hatched region: $\rho_1 = 0.13\text{GeV}^3, \rho_2 = 0$.

To make the best use of our results one could optimistically assume that $\bar{\Lambda} = 0.5 \pm 0.1$ GeV, as QCD sum rules suggest [13].⁴ Then Fig. 4.3 implies $\lambda_1 = -0.3 \pm 0.2$ GeV². It is amusing that this value for λ_1 lies exactly halfway between the two existing QCD sum rule extractions [13, 14]. However, we prefer to use the more conservative range for $\bar{\Lambda}$ and λ_1 stated in the paragraph following Eq. (4.42).

Let us apply the obtained estimates of $\bar{\Lambda}$ and λ_1 to the extraction of $|V_{cb}|$ from the total rate of the $B \rightarrow X_c \ell \bar{\nu}$ decay. The expression for the total semileptonic rate is obtained by combining Eqs. (4.29-4.31) with the perturbative order α_s correction from Ref. [39]. It is known that order $\alpha_s^2 \beta_0$ corrections to the total rate are substantial [28], therefore we include them as well. Expanding the result to order $1/\bar{m}_B^3$ yields

$$\begin{aligned} \Gamma = & \frac{|V_{cb}|^2 G_F^2 \bar{m}_B^5}{192 \pi^3} \left[0.3689 - \frac{\alpha_s}{\pi} (0.566 + 2.3 \frac{\bar{\Lambda}}{\bar{m}_B}) - 0.7 \frac{\alpha_s^2 \beta_0}{\pi^2} - 0.6080 \frac{\bar{\Lambda}}{\bar{m}_B} \right. \\ & - 0.349 \frac{\bar{\Lambda}^2}{\bar{m}_B^2} - 1.175 \frac{\lambda_1}{\bar{m}_B^2} - 2.757 \frac{\lambda_2}{\bar{m}_B^2} - 0.11 \frac{\bar{\Lambda}^3}{\bar{m}_B^3} - 1.21 \frac{\bar{\Lambda} \lambda_1}{\bar{m}_B^3} + 2.95 \frac{\bar{\Lambda} \lambda_2}{\bar{m}_B^3} \\ & \left. - 2.27 \frac{\rho_1}{\bar{m}_B^3} + 2.76 \frac{\rho_2}{\bar{m}_B^3} - 2.73 \frac{\mathcal{T}_1}{\bar{m}_B^3} + 0.55 \frac{\mathcal{T}_2}{\bar{m}_B^3} - 3.84 \frac{\mathcal{T}_3}{\bar{m}_B^3} - 2.76 \frac{\mathcal{T}_4}{\bar{m}_B^3} \right]. \end{aligned} \quad (4.43)$$

Inverting this relation with respect to $|V_{cb}|$ we obtain

$$|V_{cb}| = (42.1 \pm 2.6(\text{theor})) \times 10^{-3} \left(\frac{\text{Br}(B \rightarrow X_c \ell \bar{\nu}) 1.59 \text{ps}}{0.104 \tau_B} \right)^{1/2}, \quad (4.44)$$

where τ_B is the B lifetime (we do not distinguish between charged and neutral B mesons). To get this formula we expressed $\bar{\Lambda}$ and λ_1 as functions of R_1^{exp} , R_2^{exp} , ρ_1 , $\mathcal{T}_1 - \mathcal{T}_4$, as in Eq. (4.42). To be consistent, we included in Eqs. (4.36,4.37) corrections of order $\alpha_s^2 \beta_0$ computed in Ref. [47]:

$$\delta R_1 [\text{GeV}] = -0.082 \frac{\alpha_s^2 \beta_0}{\pi^2}, \quad \delta R_2 = -0.098 \frac{\alpha_s^2 \beta_0}{\pi^2}. \quad (4.45)$$

However, the numerical impact of these terms is very small. The “theoretical”

⁴The QCD sum rules for $\bar{\Lambda}$ seem to be on a much firmer ground than QCD sum rules for λ_1 : see Refs. [13, 14].

error in Eq. (4.44) has several sources: (i) varying the magnitude of the matrix elements $\rho_1, \mathcal{T}_1 - \mathcal{T}_4$ in the range $0 - (0.5 \text{ GeV})^3$, with ρ_1 taken to be positive; (ii) the experimental error in the values of R_1, R_2 ; (iii) the uncertainty from neglecting higher order perturbative corrections in Eq. (4.43), which was taken to be half of the $\alpha_s^2 \beta_0$ correction. All these uncertainties have comparable size. Taking $Br(B \rightarrow X_c \ell \bar{\nu}) = (10.43 \pm 0.24)\%$, $\tau_B = 1.59 \pm 0.06 \text{ ps}$ [8], we get

$$|V_{cb}| = (42.1 \pm 2.2(\text{exp}) \pm 2.6(\text{theor})) \times 10^{-3}. \quad (4.46)$$

Comparing this result with the value obtained from exclusive decays, Eq. (3.30), we see that they are marginally compatible; the corresponding χ^2 is about 2.3. Their average computed according to the ‘‘PDG rules’’ is

$$|V_{cb}| = (38.4 \pm 3.5) \times 10^{-3}. \quad (4.47)$$

Let us also translate the range obtained for $\bar{\Lambda}, \lambda_1$ into the range for the quark pole masses and $\overline{\text{MS}}$ masses. Eq. (2.15) yields the difference between the quark pole masses, $m_b - m_c = 3.38 \pm 0.09 \text{ GeV}$, where the uncertainty due to terms of order $\Lambda_{\text{QCD}}^3/m_c^2$ was estimated as $(0.5 \text{ GeV})^3/\bar{m}_D^2 \simeq 0.03 \text{ GeV}$. The quark pole masses are $m_b = 4.84 \pm 0.33 \text{ GeV}$, $m_c = 1.46 \pm 0.42 \text{ GeV}$. The $\overline{\text{MS}}$ masses to order $\alpha_s^2 \beta_0$ can be computed using the formula [56]

$$\bar{m}_Q(m_Q) = m_Q \left(1 - \frac{4\alpha_s(m_Q)}{3\pi} - 1.56 \frac{\alpha_s(m_Q)^2 \beta_0}{\pi^2} \right). \quad (4.48)$$

The result is $\bar{m}_b(m_b) = 4.05 \pm 0.27 \text{ GeV}$, $\bar{m}_c(m_c) = 0.90 \pm 0.25 \text{ GeV}$. We used $\alpha_s(m_b) = 0.22$, $\alpha_s(m_c) = 0.39$. The central value for $\bar{m}_b(m_b)$ is in good agreement with the lattice determinations $\bar{m}_b(m_b) = 4.17 \pm 0.06 \text{ GeV}$ and $\bar{m}_b(m_b) = 4.0 \pm 0.01 \text{ GeV}$ [57].

Chapter 5 Photon spectrum in the inclusive $B \rightarrow X_s \gamma$ decay

5.1 General setup

“For a Snark’s a peculiar creature, that won’t

Be caught in a commonplace way.

Do all that you know, and try all that you don’t:

Not a chance must be wasted to-day.”

Lewis Carroll [1]

The inclusive $B \rightarrow X_s \gamma$ decay has received a lot of attention in recent years [58, 59, 60, 61, 62, 63], primarily due to its sensitivity to physics beyond the Standard Model (SM) [59, 62, 63]. Like any other flavor changing neutral current process, it can only arise at one-loop level in the SM, and therefore possible new physics can yield comparable contributions. However, the recent CLEO measurement [64] excludes significant deviations from the SM.

Since the b quark is heavy compared to the QCD scale, the inclusive $B \rightarrow X_s \gamma$ decay rate can be calculated in a systematic QCD-based expansion [19, 65], modulo some caveats [66]. The decay rate computed in the $m_b \rightarrow \infty$ limit coincides with the free quark decay result. Corrections can then be included in an expansion in powers of $1/m_b$ and $\alpha_s(m_b)$.

In this chapter we show that the moments of the photon spectrum can be obtained to order α_s accuracy by a relatively simple calculation [67]. We evaluate these corrections for the first two moments of the photon spectrum. Since $B \rightarrow X_s \gamma$ is a two-body decay at the quark level (at leading order in α_s), the photon spectrum

is monochromatic in the spectator model. Therefore, the moments are also sensitive to the nonperturbative corrections in the heavy quark expansion. They provide a model-independent determination of the matrix elements $\bar{\Lambda}$ and λ_1 of the Heavy Quark Effective Theory.

The $B \rightarrow X_s \gamma$ decay in the standard model is mediated by penguin diagrams. The QCD corrections to this process form a power series in the parameter $\alpha_s \ln(M_W^2/m_b^2)$, which is too large to provide a reliable expansion. Therefore, it is convenient to integrate out the virtual top quark and W boson effects (and possible new physics) at the W scale, and sum up the large logarithms using the operator product expansion and the renormalization group. We work with the operator basis and effective Hamiltonian of Ref. [59]

$$H_{\text{eff}} = -\frac{4G_F}{\sqrt{2}} V_{ts}^* V_{tb} \sum_{i=1}^8 C_i(\mu) O_i(\mu), \quad (5.1)$$

where

$$\begin{aligned} O_1 &= (\bar{c}_{L\beta} \gamma^\mu b_{L\alpha}) (\bar{s}_{L\alpha} \gamma_\mu c_{L\beta}), & O_2 &= (\bar{c}_{L\alpha} \gamma^\mu b_{L\alpha}) (\bar{s}_{L\beta} \gamma_\mu c_{L\beta}), \\ O_7 &= \frac{e}{16\pi^2} m_b \bar{s}_{L\alpha} \sigma^{\mu\nu} F_{\mu\nu} b_{R\alpha}, & O_8 &= \frac{g}{16\pi^2} m_b \bar{s}_{L\alpha} \sigma^{\mu\nu} \lambda_{\alpha\beta}^a G_{\mu\nu}^a b_{R\beta}. \end{aligned} \quad (5.2)$$

Here α and β are color indices, and $\lambda_{\alpha\beta}^a$ are Gell-Mann matrices. Only the operators whose Wilson coefficients are of order unity are listed; the coefficients $C_3 - C_6$ of the four-quark operators $O_3 - O_6$ are about an order of magnitude smaller, since they arise only due to operator mixing. As the matrix elements of all operators except O_7 contain an overall factor of α_s (once we use the “effective” Wilson coefficients [62] defined below), we shall neglect $O_3 - O_6$. This is a very good approximation; for example, the contribution of the operators $O_3 - O_6$ to the total rate does not exceed 0.03% [68]. Furthermore, the operator O_1 does not contribute to the decay rate at one-loop level because of its color structure. Thus we only have to consider O_2, O_7 and O_8 . (When we consider nonperturbative effects, we should also include O_1 .)

The coefficients C_i are known to next-to-leading order in α_s [61]. For our purposes it is sufficient to summarize the results for the coefficients of the effective Hamiltonian

in the leading logarithmic approximation, for which we adopt the scheme independent definitions of Ref. [62]. In the Standard Model $C_2(M_W) = 1$,

$$\begin{aligned} C_7(M_W) &= \frac{3x^3 - 2x^2}{4(x-1)^4} \ln x + \frac{-8x^3 - 5x^2 + 7x}{24(x-1)^3}, \\ C_8(M_W) &= \frac{-3x^2}{4(x-1)^4} \ln x + \frac{-x^3 + 5x^2 + 2x}{8(x-1)^3}, \end{aligned} \quad (5.3)$$

where $x = m_t^2/M_W^2$. At a low scale μ , these coefficients become

$$\begin{aligned} C_2(\mu) &= \frac{1}{2} \left(\eta^{6/23} + \eta^{-12/23} \right) C_2(M_W), \\ C_7^{\text{eff}}(\mu) &= \eta^{16/23} C_7(M_W) + \frac{8}{3} \left(\eta^{14/23} - \eta^{16/23} \right) C_8(M_W) + C_2(M_W) \sum_{i=1}^8 h_i \eta^{a_i}, \\ C_8^{\text{eff}}(\mu) &= \eta^{14/23} C_8(M_W) + C_2(M_W) \sum_{i=1}^5 g_i \eta^{b_i}, \end{aligned} \quad (5.4)$$

where $\eta = \alpha_s(M_W)/\alpha_s(\mu)$, and the numerical values of the h_i 's, g_i 's, a_i 's, and b_i 's can be found in Ref. [62]. The scale is usually chosen to be $\mu = m_b$, and one estimates the uncertainties related to the unknown higher order terms by varying μ , typically between $m_b/2$ and $2m_b$. However, our results will be scale independent to order α_s , so this is not going to be a large uncertainty.

Since experimentally one needs to make a lower cut on the photon energy, we define moments of the photon spectrum as

$$M_n(E_0) = \frac{\int_{E_0}^{E_\gamma^{\text{max}}} E_\gamma^n \frac{d\Gamma}{dE_\gamma} dE_\gamma}{\int_{E_0}^{E_\gamma^{\text{max}}} \frac{d\Gamma}{dE_\gamma} dE_\gamma}. \quad (5.5)$$

Here $E_\gamma^{\text{max}} = [M_B^2 - (M_K + M_\pi)^2]/2M_B$ is the maximal possible photon energy.

Let us show that in order to compute the moments of the photon spectrum to order α_s it is sufficient to use the coefficients C_2, C_7, C_8 in the leading logarithmic approximation. To illustrate our argument, we denote schematically the contribution of a given operator O_i to the n -th moment of the spectrum by $\langle O_i \rangle_n$. Then the moments

M_n may be rewritten as

$$M_n \sim \left| \frac{C_7^{\text{eff}} \langle O_7 \rangle_n + C_8^{\text{eff}} \langle O_8 \rangle_n + C_2 \langle O_2 \rangle_n}{C_7^{\text{eff}} \langle O_7 \rangle_0 + C_8^{\text{eff}} \langle O_8 \rangle_0 + C_2 \langle O_2 \rangle_0} \right|^2 = \left| \frac{\langle O_7 \rangle_n + \frac{C_8^{\text{eff}}}{C_7^{\text{eff}}} \langle O_8 \rangle_n + \frac{C_2}{C_7^{\text{eff}}} \langle O_2 \rangle_n}{\langle O_7 \rangle_0 + \frac{C_8^{\text{eff}}}{C_7^{\text{eff}}} \langle O_8 \rangle_0 + \frac{C_2}{C_7^{\text{eff}}} \langle O_2 \rangle_0} \right|^2. \quad (5.6)$$

For $i \neq 7$, the contributions $\langle O_i \rangle_n$ are of order α_s . The reason for this is that in the scheme independent approach of Ref. [62] the order α_s^0 contributions from the four-quark operators $O_1 - O_6$ are absorbed into C_7, C_8 . Therefore, to determine the NLO corrections to M_n , one has to take into account the order α_s contributions from $\langle O_2 \rangle_n, \langle O_8 \rangle_n$, as well as the contribution from $\langle O_7 \rangle_n$ to order α_s . It is sufficient to know the Wilson coefficients C_i only to leading log accuracy.¹

The other important observation is that the virtual corrections to the matrix elements of the operators O_2, O_7, O_8 do not contribute to the moments of the photon spectrum at order α_s . The reason is that the virtual corrections to the photon spectrum yield only terms proportional to $\delta(E_\gamma - E_\gamma^{\text{max}})$, and therefore they contribute equally to the numerator and the denominator of Eq. (5.5). Thus, these contributions cancel to order α_s in the moments M_n . Consequently, only the Bremsstrahlung corrections have to be computed.

5.2 Order α_s perturbative corrections

In this section we study the perturbative corrections to the photon spectrum in the free quark decay, or parton, model. As discussed in more detail in the next section, the nonperturbative corrections to the parton model are suppressed by $1/m_{b,c}^2$.

Following Ref. [69] the strange quark mass is kept finite to regularize collinear divergences. We use the $\overline{\text{MS}}$ subtraction scheme, Feynman gauge, and dimensional regularization for infrared and ultraviolet divergences, and phase-space integrals as

¹The fact that one needs to know C_i only to the leading log accuracy to compute the moments at order α_s was emphasized in Ref. [67] because at that time the NLO computation of C_i was not available.

well. The quantity that is simple to calculate in perturbation theory is

$$\delta m_n(x_0) = \frac{\int_{x_0}^1 (x^n - 1) \frac{d\Gamma_{\text{FQDM}}}{dx} dx}{\int_{x_0}^1 \frac{d\Gamma_{\text{FQDM}}}{dx} dx}, \quad (5.7)$$

where Γ_{FQDM} denotes the decay rate in the free quark decay model, and the dimensionless parameters

$$x = \frac{2E_\gamma}{(1-r)m_b}, \quad r = \frac{m_s^2}{m_b^2} \quad (5.8)$$

were introduced. The variable x corresponds to $E_\gamma/E_\gamma^{\text{max}}$ in the free quark decay model. The definition (5.7) makes it apparent that the functions $\delta m_n(x_0)$ are proportional to α_s and that they are not affected by corrections proportional to $\delta(1-x)$ at this order. In the next section we shall discuss how to relate δm_n to the experimentally measurable moments M_n .

It turns out that near the end point of the photon spectrum only the operators O_2 and O_7 are important [69, 67]. We are mainly interested in the experimentally accessible region of the photon energy, which is above 1.8 GeV. Therefore O_8 will be neglected altogether in what follows.²

The contributions coming from the square of O_2 and the interference of O_2 and O_7 are regular functions of the photon energy, and their explicit form can be found in Refs. [69, 68]. The only singular (and numerically the most significant) contribution to the the free quark decay rate Γ_{FQDM} at order α_s comes from the operator O_7 alone. In the $r \rightarrow 0$ limit this contribution reads

$$\begin{aligned} \frac{d\Gamma_{77}}{dx} &= \Gamma_0 \left[\frac{m_b(\mu)}{m_b} \right]^2 \left\{ \left[1 - \frac{\alpha_s C_F}{4\pi} \left(5 + \frac{4}{3} \pi^2 - 2 \ln \frac{m_b^2}{\mu^2} \right) \right] \delta(1-x) \right. \\ &\quad \left. + \frac{\alpha_s C_F}{4\pi} \left[7 + x - 2x^2 - 2(1+x) \ln(1-x) - \left(\frac{7}{1-x} + 4 \frac{\ln(1-x)}{1-x} \right)_+ \right] \right\}, \end{aligned} \quad (5.9)$$

²Away from the end point the contribution of O_8 becomes significant, and even dominates the spectrum below about 1.2 GeV [70].

		$x_0 = 0.91$	$x_0 = 0.83$	$x_0 = 0.75$
$\delta m_1(x_0)$	$r = 4 \cdot 10^{-4}$	-0.014	-0.020	-0.025
	$r = 1 \cdot 10^{-2}$	-0.012	-0.017	-0.020
$\delta m_2(x_0)$	$r = 4 \cdot 10^{-4}$	-0.028	-0.040	-0.046
	$r = 1 \cdot 10^{-2}$	-0.023	-0.032	-0.038

Table 5.1: Central values of $\delta m_1(x_0)$ and $\delta m_2(x_0)$ for two different values of m_s . $r = 4 \cdot 10^{-4}$ corresponds to $m_s = 100$ MeV, while $r = 1 \cdot 10^{-2}$ corresponds to a constituent quark mass $m_s = 500$ MeV. For $m_b \simeq 4.8$ GeV, $x_0 = 0.91$, $x_0 = 0.83$ and $x_0 = 0.75$ correspond to $E_0 = 2.2$ GeV, $E_0 = 2.0$ GeV and $E_0 = 1.8$ GeV, respectively.

where $C_F = 4/3$ for $SU(3)$, and

$$\Gamma_0 = \frac{G_F^2 |V_{tb} V_{ts}^*|^2 \alpha C_7^{\text{eff}}(\mu)^2}{32 \pi^4} m_b^5. \quad (5.10)$$

We only explicitly presented the corrections in the $r \rightarrow 0$ limit, but we included the r -dependent terms in our numerical results. The $(f(x))_+$ distribution corresponding to the function $f(x)$ acts on a test function $g(x)$ as

$$\int_0^1 (f(x))_+ g(x) dx = \int_0^1 f(x) [g(x) - g(1)] dx. \quad (5.11)$$

The α_s correction in Eq. (5.9) modifies the prediction for the total decay rate by about 15%, while it affects the first two moments of the photon spectrum, M_1 and M_2 , by less than 3% and 5%, respectively. Our numerical results for δm_1 and δm_2 , including the contribution of O_2 , are shown in Table 5.1.

When evaluating these corrections, it has to be kept in mind that the perturbative expansion becomes singular in the photon end point region, and a resummation of the perturbative corrections may be required. Since we are interested in the moments M_n for small n , and since the exponent of the Sudakov factor that suppresses the spectrum near the end point [71] becomes of order unity only around $x \sim 0.99$, our calculation is consistent without taking these effects into account.

5.3 Nonperturbative corrections

The problem of computing nonperturbative corrections to the inclusive $B \rightarrow X_s \gamma$ decay is a subtle one. Although it has been extensively discussed in the literature [65, 66], a complete understanding of the nonperturbative effects is still lacking. Here we limit ourselves to the most elementary discussion.

It is easy to include the leading nonperturbative contributions if only the operator O_7 is retained [65]. Then the moments of the photon spectrum can be evaluated using OPE and the hypothesis of local quark-hadron duality, along the lines of Section 2.2. One considers the expectation value of the time-ordered product

$$T_{\mu\nu}^{\alpha\beta}(q \cdot v) = -i \int d^4x e^{-iq \cdot x} \langle B(v) | T [\bar{b}_R \sigma^{\alpha\beta} s_L(x), \bar{s}_L \sigma_{\mu\nu} b_R(0)] | B(v) \rangle, \quad (5.12)$$

where q^2 is fixed to zero. The analytic structure of $T(q \cdot v)$ is shown in Fig. 5.1. The total decay rate and the moments of the photon spectrum can be obtained by integrating the product of $T(q \cdot v)$ with an appropriate smooth weight function along the contour C in Fig. 5.1. As usual, away from the cut T can be computed using the OPE. If the point $q \cdot v = E_0$ where the contour approaches the cut is far away from the end point, $q \cdot v = E_\gamma^{max}$, the use of the OPE near $q \cdot v = E_0$ can be justified by the local quark-hadron duality. The upshot is that the moments of the photon spectrum in Eq. (5.5) are calculable provided E_0 is sufficiently small. Here “sufficiently small” means that the invariant mass of the corresponding hadronic final state, $m_{X_s}(E_0) = \sqrt{m_B(m_B - 2E_0)}$, must be much larger than Λ_{QCD} .

The OPE computation of the $B \rightarrow X_s \gamma$ decay in the HQET framework was first performed in Ref. [65]. As expected, the leading contribution is given by the parton model result, while the leading nonperturbative corrections are parametrized by the HQET matrix elements λ_1 and λ_2 . Again we present the resulting corrections to the photon spectrum only in the $r \rightarrow 0$ limit:

$$\frac{d\Gamma}{dx} = \Gamma_0 \left(1 + \frac{\lambda_1 - 9\lambda_2}{2m_b^2} \right) \left[\delta(1-x) - \frac{\lambda_1 + 3\lambda_2}{2m_b^2} \delta'(1-x) - \frac{\lambda_1}{6m_b^2} \delta''(1-x) \right]. \quad (5.13)$$

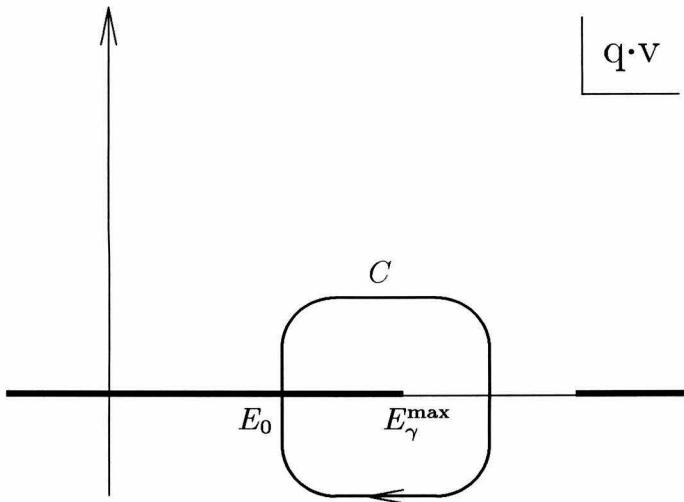


Figure 5.1: The analytic structure of the time-ordered product relevant for the $B \rightarrow X_s \gamma$ decay. The moments of the photon spectrum with lower limit E_0 can be obtained by integrating $T(q \cdot v)$ with an appropriate weight along the contour C .

If the four-quark operators O_1 and O_2 are included, the situation becomes much more complicated. Strictly speaking, the contribution of O_1, O_2 (including their interference with O_7) cannot be computed in the OPE for the physical value of m_c . If the charm quark were heavier, one could integrate it out, and then use the OPE to compute the contribution of O_1, O_2 . This has been done in Ref. [66]. It turns out that the leading nonperturbative correction is suppressed only by $\Lambda_{\text{QCD}}^2/m_c^2$ and is parametrized by a single nonperturbative matrix element λ_2 . Assuming that this result continues to hold even for the physical value of m_c , one can estimate the size of this nonperturbative correction to the total $B \rightarrow X_s \gamma$ rate. It turns out to be small, but not completely negligible: about 3%. Unfortunately, higher order nonperturbative corrections to this result are suppressed only by powers of $m_b \Lambda_{\text{QCD}}/m_c^2 \sim 0.6$ [66]. This means that they are not much smaller than the leading nonperturbative contribution. The conclusion is that there are uncalculable nonperturbative corrections to the $B \rightarrow X_s \gamma$ decay of order 2% originating from O_1, O_2 . One should take this estimate with a grain of salt, however, since for the physical values of m_c the charm

on the photon energy. For example, $E_0 = 2 \text{ GeV}$ or $E_0 = 1.8 \text{ GeV}$ would correspond to $M_{X_s} < 2.6 \text{ GeV}$ or $M_{X_s} < 3 \text{ GeV}$, respectively. Varying E_0 provides a check on the systematic uncertainties: the extracted values of $\bar{\Lambda}$ and λ_1 should be unaffected by the variations of E_0 once the corresponding hadronic invariant mass is sufficiently above the resonance region.

5.4 Extracting HQET parameters from the moments of the photon spectrum

We can summarize our discussion by writing the theoretical prediction for the first two moments of the photon spectrum as

$$M_1(E_0) = \frac{M_B - \bar{\Lambda}}{2} \left[1 + \delta m_1 \left(\frac{2E_0}{m_b} \right) + \mathcal{O} \left(\alpha_s^2, \alpha_s \frac{\Lambda^2}{m_b^2}, \frac{\Lambda^3}{m_b^3} \right) \right], \quad (5.16)$$

$$M_2(E_0) - M_1(E_0)^2 = -\frac{\lambda_1}{12} + \left(\frac{m_b}{2} \right)^2 \left[\delta m_2 \left(\frac{2E_0}{m_b} \right) - 2 \delta m_1 \left(\frac{2E_0}{m_b} \right) + \mathcal{O} \left(\alpha_s^2, \alpha_s \frac{\Lambda^2}{m_b^2}, \frac{\Lambda^3}{m_b^3} \right) \right]. \quad (5.17)$$

Λ denotes some QCD scale of order Λ_{QCD} or $\bar{\Lambda}$. To the order these relations are accurate, it is consistent to replace m_b by $M_B - \bar{\Lambda}$ everywhere in Eqs. (5.16,5.17). The numerical results for $\delta m_1(x_0)$ and $\delta m_2(x_0)$ are listed in Table 5.1 for three different values of x_0 .

The significance of the relation Eq. (5.16) is that it provides a reliable means of determining $\bar{\Lambda}$. The relation Eq. (5.17) is less useful, since the effect of λ_1 on the second moment is similar in size to the possible effect of the uncalculable nonperturbative corrections from O_1, O_2 .

The main theoretical uncertainties in this measurement of $\bar{\Lambda}$ are due to nonperturbative corrections from O_1, O_2 and the higher order perturbative corrections to M_1 . The former are of order 2%, as discussed above. The latter are harder to estimate. A very naive estimate would be $(\alpha_s(m_b)/\pi)^2 \sim 0.005$. However, this does not take into account a possible numerical coefficient. Ideally one would like to know the size

of order $\alpha_s^2\beta_0$ corrections to the moments, but the corresponding calculation has not been performed. Therefore we will assume that higher order perturbative corrections are not larger than the order α_s corrections shown in Table 5.1, i.e., 1 – 2%. Thus the total theoretical uncertainty in the value of M_1 is about 3%. The corresponding uncertainty in $\bar{\Lambda}$, according to Eq. (5.16), is about 0.15 GeV.

We would like to emphasize that the left-hand sides of the relations Eqs. (5.16,5.17) are measurable at CLEO; in fact, the central values can be extracted from Ref. [64]. As we do not know the cross-correlations of the errors on the data points, we are not in a position to quote numerical values for the experimental uncertainties. From the central values of the data, solving the equation Eq. (5.16), we find (with large uncertainties)

$$\bar{\Lambda} \sim 450 \text{ MeV}, \quad m_b \sim 4.83 \text{ GeV}. \quad (5.18)$$

This value is in agreement with the QCD sum rule determination of $\bar{\Lambda}$ [13], $\bar{\Lambda} = 0.5 \pm 0.1$ GeV. It is also consistent with the range of values for $\bar{\Lambda}$ obtained in Section 4.2 from the analysis of the lepton spectrum in the $B \rightarrow X_c \ell \bar{\nu}$ decay.

In view of our earlier discussion, it is important to try to expand the experimental signal region. On the one hand, the systematic uncertainties inherent in our analysis (related to how well the quark-hadron duality holds) can be estimated by varying the lower cut on the photon energy, as discussed at the end of Section 5.3. On the other hand, expanding the signal region would diminish the sensitivity of the results as to whether the Sudakov logarithms at the end point are resummed or not.

The sensitivity of the moments of the spectrum to new physics is limited by how much operators other than O_7 affect M_n . We found that O_2 does not contribute to δm_1 and δm_2 by more than 10% in the SM. Given that the experimental constraint on the total decay rate from CLEO excludes large deviations from the SM, we conclude that the moments are largely insensitive to new physics. Even if physics beyond the SM contributes to the $B \rightarrow X_s \gamma$ decay, the proposed determination of $\bar{\Lambda}$ and λ_1 is likely to remain unaffected.

We conclude that the measurement of the moments of the photon spectrum in the

inclusive $B \rightarrow X_s \gamma$ decay will provide a measurement of $\bar{\Lambda}$, which in turn will refine theoretical predictions for other observables in heavy quark decays. In particular, the accuracy of the extraction of the CKM angle $|V_{cb}|$ along the lines of Section 4.2 could be improved.

Chapter 6 Concluding remarks

“The rest of my speech” (he explained to his men)

“You shall hear when I’ve leisure to speak it.

But the Snark is at hand, let me tell you again!

’Tis you glorious duty to seek it!”

Lewis Carroll [1]

We have described two methods of measuring the CKM matrix element $|V_{cb}|$: from the differential rate of the exclusive decay $B \rightarrow D^* \ell \bar{\nu}$, and from the total rate of the inclusive semileptonic decay $B \rightarrow X_c \ell \bar{\nu}$. Both methods are model-independent, i.e., based only on the genuine predictions of QCD for the hadronic matrix elements. The “exclusive” method has intrinsic theoretical uncertainty of order 3 – 6% coming from Heavy Quark Symmetry violations. Zero recoil sum rules can, in principle, tell us if these violations are anomalously large. However this requires knowing the HQET parameter λ_1 , whose value is very uncertain at present. The “inclusive” method of measuring $|V_{cb}|$ can potentially be more accurate. The problem there is that the quark masses m_c and m_b , or equivalently the HQET parameters $\bar{\Lambda}$ and λ_1 , are still poorly known. As shown in Chapter 4, studying the lepton spectrum in the $B \rightarrow X_c \ell \bar{\nu}$ decay allows us, in principle, to pin down both of them. In practice, the lepton spectrum is sensitive only to a particular linear combination of $\bar{\Lambda}$ and λ_1 , the “othogonal” linear combination being only weakly constrained by the data. Thus our results, $\bar{\Lambda} = 0.45 \pm 0.3$ GeV, $\lambda_1 = -0.25 \pm 0.35$ GeV², have rather large uncertainties. The corresponding quark pole masses are $m_b = 4.84 \pm 0.33$ GeV, $m_c = 1.46 \pm 0.42$ GeV. (The difference $m_b - m_c$ is known to a much better accuracy: $m_b - m_c = 3.38 \pm 0.09$ GeV.) Consequently, the inclusive determination of $|V_{cb}|$ has a theoretical uncertainty of about 6% (see Eq. (4.44)).

The accuracy of the inclusive determination of $|V_{cb}|$ could be significantly improved if the values of the heavy quark masses were better known. One way to accomplish this is to measure the photon spectrum in the inclusive $B \rightarrow X_s \gamma$ decay near its end point. As shown in Chapter 5, the moments of the spectrum are sensitive to the HQET parameter $\bar{\Lambda}$. This measurement could yield a value for m_b accurate to within 150 MeV. The major theoretical uncertainty here is the unknown order α_s^2 corrections to the moments. A calculation of the order $\alpha_s^2 \beta_0$ contributions to the moments is, therefore, desirable.

Other methods of extracting heavy quark masses, of course, exist. A very attractive idea is to use the measurement of the cross-section $e^+e^- \rightarrow b\bar{b}$ near the $B\bar{B}$ threshold [15]. However, the data exist only for energies up to 600 MeV above the threshold, which makes the comparison of the data with the theory next to impossible [72].

Coming back to the determination of $|V_{cb}|$, the limiting factor in the inclusive measurement is, ultimately, the unknown higher order perturbative corrections for the total $B \rightarrow X_c \ell \bar{\nu}$ rate. The presumably dominant part of the two-loop contribution, the $\alpha_s^2 \beta_0$ contribution, has been calculated [28], and progress towards a complete two-loop calculation has been made [52]. However, one may say with confidence that computing order α_s^3 corrections will remain beyond human capabilities for years to come. The theoretical uncertainty in the value of $|V_{cb}|$ coming from the latter corrections is about 2%. Thus, optimistically, one may hope to reduce the current error bars by a factor of three.

Bibliography

- [1] Lewis Carroll, *The Hunting of the Snark*, Simon and Schuster, 1962.
- [2] D.J. Gross and F. Wilczek, *Phys. Rev. Lett.* 30 (1973) 1343; H.D. Politzer, *Phys. Rev. Lett.* 30 (1973) 1346.
- [3] N. Isgur and M.B. Wise, *Phys. Lett.* B232 (1989) 113; *Phys. Lett.* B237 (1990) 527.
- [4] J.D. Bjorken and S. Drell, *Relativistic quantum mechanics*, McGraw-Hill, 1964.
- [5] E. Eichten and B. Hill, *Phys. Lett.* B234 (1990) 511; H. Georgi, *Phys. Lett.* B240 (1990) 447.
- [6] M. Luke and A.V. Manohar, *Phys. Lett.* B286 (1992) 348; Yu-Qi Chen, *Phys. Lett.* B317 (1993) 421; W. Kilian and T. Ohl, *Phys. Rev.* D50 (1994) 4649; M. Finkemeier, H. Georgi, and M. McIrvin, preprint HUTP-96-A053 [[hep-ph/9701243](#)], to be published in *Phys. Rev. D*; R. Sundrum, preprint BUHEP-97-14 [[hep-ph/9704256](#)].
- [7] G.P. Lepage and B.A. Thacker, *Nucl. Phys. B (Proc. Suppl.)* 4 (1988) 199; E. Eichten and B. Hill, *Phys. Lett.* B243 (1990) 427; A.F. Falk, B. Grinstein, and M.E. Luke, *Nucl. Phys.* B357 (1991) 185.
- [8] L. Montanet *et al.*, *Review of Particle Properties*, *Phys. Rev.* D54 (1996) 1.
- [9] I.I. Bigi, M.A. Shifman, N.G. Uraltsev, and A.I. Vainshtein, *Phys. Rev.* D52 (1995) 196.
- [10] S. Balk, J.G. Körner, and D. Pirjol, *Nucl. Phys.* B428 (1994) 499.
- [11] M. Gremm and A. Kapustin, preprint CALT-68-2042 [[hep-ph/9603448](#)], to be published in *Phys. Rev. D*.

- [12] A.L. Fetter and J.D. Walecka, *Quantum theory of many-particle systems*, McGraw-Hill, 1971.
- [13] E. Bagan, P. Ball, V.M. Braun, and H.G. Dosch, *Phys. Lett.* B278 (1992) 457.
- [14] M. Neubert, *Phys. Lett.* B389 (1996) 727.
- [15] M.B. Voloshin and Yu.M. Zaitsev, *Sov. Phys. Usp.* 30 (1987) 553; M. B. Voloshin, *Int. J. Mod. Phys. A*10 (1995) 2865; L.J. Reinders, *Phys. Rev.* D38 (1988) 947; M. Jamin and A. Pich, preprint IFIC-97-06 [hep-ph/9701353].
- [16] Z. Ligeti and M.B. Wise, *Phys. Rev.* D53 (1996) 4937.
- [17] A.F. Falk, H. Georgi, B. Grinstein, and M.B. Wise, *Nucl. Phys.* B343 (1990) 1; J.D. Bjorken, *Proceedings of the 18th SLAC Summer Institute on Particle Physics*, pp. 167, Stanford, July 1990, ed. by J.F. Hawthorne (SLAC, Stanford, 1991); A.F. Falk, *Nucl. Phys.* B378 (1992) 79.
- [18] N. Cabibbo, G. Corbo, and L. Maiani, *Nucl. Phys.* B155 (1979) 93; G. Altarelli, N. Cabibbo, G. Gorbo, L. Maiani, and G. Martinelli, *Nucl. Phys.* B208 (1982) 365.
- [19] J. Chay, H. Georgi, and B. Grinstein, *Phys. Lett.* B247 (1990) 399.
- [20] I.I. Bigi, N.G. Uraltsev, and A.I. Vainshtein, *Phys. Lett.* B293 (1992) 430 [(E) *Phys. Lett.* B297 (1993) 477]; I.I. Bigi, M. Shifman, N.G. Uraltsev, and A. Vainshtein, *Phys. Rev. Lett.* 71 (1993) 496;
- [21] E.C. Poggio, H.R. Quinn, and S. Weinberg, *Phys. Rev.* D13 (1976) 1958.
- [22] F.J. Dyson, *Phys. Rev.* 85 (1952) 861.
- [23] J. Fischer, hep-ph/9704351.
- [24] M.A. Shifman, A.I. Vainshtein, and V.I. Zakharov, *Nucl. Phys.* B147 (1979) 385.
- [25] M. Neubert, *Phys. Lett.* B338 (1994) 84.

- [26] A. Kapustin, Z. Ligeti, M.B. Wise, and B. Grinstein, Phys. Lett. B375 (1996) 327.
- [27] A. Czarnecki, Phys. Rev. Lett. 76 (1996) 4124.
- [28] M. Luke, M.J. Savage, and M.B. Wise, Phys. Lett. B343 (1995) 329; Phys. Lett. B345 (1995) 301;
- [29] M.E. Luke, Phys. Lett. B252 (1990) 447.
- [30] L. Randall and M.B. Wise, Phys. Lett. B303 (1993) 135.
- [31] B. Blok, L. Koyrakh, M. Shifman, and A.I. Vainshtein, Phys. Rev. D49 (1994) 3356.
- [32] J.G. Korner, K. Melnikov, and O. Yakovlev, hep-ph/9502377.
- [33] B.H. Smith and M.B. Voloshin, Phys. Lett. B340 (1994) 176.
- [34] S.J. Brodsky, G.P. Lepage, and P.B. Mackenzie, Phys. Rev. D28 (1983) 228.
- [35] M. Gremm, A. Kapustin, Z. Ligeti, and M.B. Wise, Phys. Rev. Lett. 77 (1996) 20.
- [36] N. Isgur, D. Scora, B. Grinstein, and M. Wise, Phys. Rev. D39 (1989) 799; D. Scora and N. Isgur, Phys. Rev. D52 (1995) 2783.
- [37] D. Buskulic *et al.*, ALEPH collaboration, preprint CERN-PPE-96-150.
- [38] B. Barish *et al.*, CLEO collaboration, Phys.Rev. D51 (1995) 1014.
- [39] M. Jezabek and J.H. Kuhn, Nucl. Phys. B320 (1989) 20; A. Czarnecki and M. Jezabek, Nucl. Phys. B427 (1994) 3.
- [40] A.F. Falk, M. Luke, and M.J. Savage, Phys. Rev. D53 (1996) 2491.
- [41] A.V. Manohar and M.B. Wise, Phys. Rev. D49 (1994) 1310.
- [42] T. Mannel, Nucl. Phys. B413 (1994) 396.

- [43] J. Bartelt *et al.*, CLEO Collaboration, CLEO/CONF 93-19.
- [44] B. Barish *et al.*, CLEO Collaboration, Phys. Rev. Lett. 76 (1996) 1570.
- [45] T. Mannel, Phys. Rev. D50 (1994) 428.
- [46] B. Blok, R. Dikeman, and M. Shifman, Phys. Rev. D51 (1995) 6167.
- [47] M. Gremm and I. Stewart, Phys. Rev. D55 (1997) 1226.
- [48] R. Wang, Ph.D. Thesis, University of Minnesota (1994).
- [49] D. Atwood and W.J. Marciano, Phys. Rev. D41 (1990) 1736.
- [50] Y. Kubota *et al.*, CLEO Collaboration, Nucl. Instr. and Meth. A320 (1992) 66.
- [51] R. Wang, private communications.
- [52] A. Czarnecki and K. Melnikov, preprint TTP-97-05 [hep-ph/9703291].
- [53] M.A. Shifman and M.B. Voloshin, Sov. J. Nucl. Phys. 45 (1987) 292; M.B. Voloshin, N.G. Uraltsev, V.A. Khoze, and M.A. Shifman, Sov. J. Nucl. Phys. 46 (1987) 112.
- [54] I.I. Bigi, M. Shifman, N.G. Uraltsev, and A. Vainshtein, Int. J. Mod. Phys. A9 (1994) 2467.
- [55] C.K. Chow and D. Pirjol, Phys. Rev. D53 (1996) 3998.
- [56] N. Gray, D.J. Broadhurst, W. Grafe, and K. Schilcher, Z. Phys. C48 (1990) 673.
- [57] M. Crisafulli *et al.*, Nucl. Phys. B457 (1995) 594; C. Davies *et al.*, Phys. Rev. Lett. 73 (1994) 2654.
- [58] S. Bertolini, F. Borzumati, and A. Masiero, Phys. Rev. Lett. 59 (1987) 180; N.G. Deshpande *et al.*, Phys. Rev. Lett. 59 (1987) 183.
- [59] B. Grinstein, R. Springer, and M.B. Wise, Phys. Lett. B202 (1988) 138; Nucl. Phys. B339 (1990) 269.

- [60] M. Misiak, Phys. Lett. B269 (1991) 161; M. Ciuchini *et al.*, Phys. Lett. B316 (1993) 127.
- [61] A.J. Buras, M. Jamin, M.E. Lautenbacher, and P.H. Weisz, Nucl. Phys. B370 (1992) 69; M. Misiak and M. Münz, Phys. Lett. B344 (1995) 308.
- [62] A.J. Buras, M. Misiak, M. Münz, and S. Pokorski, Nucl. Phys. B424 (1994) 374, and references therein.
- [63] See, for example: B. Grinstein and M.B. Wise, Phys. Lett. B201 (1988) 274; S. Bertolini, F. Borzumati, A. Masiero, and G. Ridolfi, Nucl. Phys. B353 (1991) 591; Y. Grossman and Y. Nir, Phys. Lett. B313 (1993) 126; J.L. Hewett, SLAC-PUB-6521, hep-ph/9406302.
- [64] M.S. Alam *et al.*, CLEO collaboration, Phys. Rev. Lett. 74 (1995) 2885.
- [65] A.F. Falk, M. Luke, and M.J. Savage, Phys. Rev. D49 (1994) 3367; M. Neubert, Phys. Rev. D49 (1994) 4623; I. Bigi *et al.*, in *The Fermilab Meeting*, Proc. of the Annual Meeting of the DPS of the APS, ed. C. Albright *et al.* (World Scientific, Singapore, 1993), p. 610.
- [66] M.B. Voloshin, preprint TPI-MINN-96-30-T [hep-ph/9612483]; Z. Ligeti, L. Randall, and M.B. Wise, preprint CALT-68-2097 [hep-ph/9702322]; A.K. Grant, A.G. Morgan, S. Nussinov, and R.D. Peccei, preprint UCLA-97-TEP-5 [hep-ph/9702380].
- [67] A. Kapustin and Z. Ligeti, Phys. Lett. B355 (1995) 318.
- [68] N. Pott, Phys. Rev. D54 (1996) 938.
- [69] A. Ali and C. Greub, Z. Phys. C49 (1991) 431; Phys. Lett. B259 (1991) 182; Phys. Lett. B287 (1992) 191.
- [70] A. Kapustin, Z. Ligeti, and H. David Politzer, Phys. Lett. B357 (1995) 653.

- [71] G.P. Korchemsky and A.V. Radyushkin, Phys. Lett. B279 (1992) 359; G.P. Korchemsky and G. Sterman, Phys. Lett. B340 (1994) 96.
- [72] A.H. Hoang, preprint UCSD-PTH-97-04 [hep-ph/9702331], preprint UCSD-PTH-97-08 [hep-ph/9703404]; M. Gremm and A. Kapustin, unpublished.